AMERICAN JOURNAL OF PHYSIOLOGY
HEART AND CIRCULATORY PHYSIOLOGY

Am J Physiol Heart Circ Physiol 322: H493–H522, 2022.
First published December 24, 2021; doi:10.1152/ajpheart.00392.2021

REVIEW

Vascular Biology and Microcirculation

Assessing hemodynamics from the photoplethysmogram to gain insights into vascular age: a review from VascAgeNet

Peter H. Charlton,[1,2] Birutė Paliakaitė,[3] Kristjan Pilt,[4] Martin Bachler,[5] Serena Zanelli,[6,7] Dániel Kulin,[8,9] John Allen,[10,11] Magid Hallab,[7,12] Elisabetta Bianchini,[13] Christopher C. Mayer,[5] Dimitrios Terentes-Printzios,[14] Verena Dittrich,[15] Bernhard Hametner,[5] Dave Veerasingam,[16] Dejan Žikić,[17]* and Vaidotas Marozas[3]* on behalf of VascAgeNet

[1]*Department of Public Health and Primary Care, University of Cambridge, Cambridge, United Kingdom;* [2]*Research Centre for Biomedical Engineering, University of London, London, United Kingdom;* [3]*Biomedical Engineering Institute, Kaunas University of Technology, Kaunas, Lithuania;* [4]*Department of Health Technologies, Tallinn University of Technology, Tallinn, Estonia;* [5]*Biomedical Systems, Center for Health and Bioresources, AIT Austrian Institute of Technology, Seibersdorf, Austria;* [6]*Laboratoire Analyze, Géométrie et Applications, University Sorbonne Paris Nord, Paris, France;* [7]*Axelife, Redon, France;* [8]*Institute of Translational Medicine, Semmelweis University, Budapest, Hungary;* [9]*E-Med4All Europe, Limited, Budapest, Hungary;* [10]*Research Centre for Intelligent Healthcare, Coventry University, Coventry, United Kingdom;* [11]*Faculty of Medical Sciences, Newcastle University, Newcastle upon Tyne, United Kingdom;* [12]*Centre de recherche et d'Innovation, Clinique Bizet, Paris, France;* [13]*Institute of Clinical Physiology, CNR, Pisa, Italy;* [14]*Hypertension and Cardiometabolic Unit, First Department of Cardiology, Hippokration Hospital, Medical School, National and Kapodistrian University of Athens, Athens, Greece;* [15]*Redwave Medical, Gesellschaft mit beschränkter Haftung, Jena, Germany;* [16]*Department of Cardiothoracic Surgery, Galway University Hospitals, Galway, Ireland; and* [17]*Faculty of Medicine, Institute of Biophysics, University of Belgrade, Belgrade, Serbia*

Abstract

The photoplethysmogram (PPG) signal is widely measured by clinical and consumer devices, and it is emerging as a potential tool for assessing vascular age. The shape and timing of the PPG pulse wave are both influenced by normal vascular aging, changes in arterial stiffness and blood pressure, and atherosclerosis. This review summarizes research into assessing vascular age from the PPG. Three categories of approaches are described: *1*) those which use a single PPG signal (based on pulse wave analysis), *2*) those which use multiple PPG signals (such as pulse transit time measurement), and *3*) those which use PPG and other signals (such as pulse arrival time measurement). Evidence is then presented on the performance, repeatability and reproducibility, and clinical utility of PPG-derived parameters of vascular age. Finally, the review outlines key directions for future research to realize the full potential of photoplethysmography for assessing vascular age.

arterial stiffness; arteriosclerosis; atherosclerosis; blood pressure; photoplethysmography; pulse wave velocity

INTRODUCTION

Vascular age is an emerging indicator of cardiovascular health that is indicative of cardiovascular risk, and can prompt clinical intervention (1). The function and structure of blood vessels naturally degrade with age (2). This process, known as vascular aging, includes an increase in the stiffness and diameter of the larger arteries and lengthening of the proximal aorta (3, 4). It can ultimately result in damage to the heart, kidney, and brain (1). Indicators of vascular aging have been found to be predictive of cardiovascular morbidity and all-cause mortality, such as the assessment of aortic stiffness by carotid-femoral pulse wave velocity (as assessed using applanation tonometry or vascular ultrasonography) (5). Other indicators are routinely used for diagnosis, such as the ankle-brachial index being used to diagnose peripheral arterial disease (PAD). Consequently, it is helpful to identify individuals with early vascular aging for clinical intervention (6): those whose vascular age (apparent age of the blood vessels) is greater than their chronological age (time since birth).

* D. Žikić and V. Marozas contributed equally to this work.
Correspondence: P. H. Charlton (pc657@medschl.cam.ac.uk).
Submitted 20 July 2021 / Revised 21 December 2021 / Accepted 21 December 2021

0363-6135/22 Copyright © 2022 The Authors. Licensed under Creative Commons Attribution CC-BY 4.0.
Published by the American Physiological Society.

Downloaded from journals.physiology.org/journal/ajpheart (193.219.170.065) on March 9, 2022.

However, many current approaches to assess vascular age are not yet widely used, in part due to the need for a trained operator and standardized measurement conditions.

Photoplethysmography-based devices could provide a more convenient approach to assess vascular age. Photoplethysmography is an optical technique that captures the pulsatile change in vascular blood volume with each heartbeat. It is widely used in physiological monitoring, from its use in pulse oximeters for oxygen saturation assessment (7), to its use in toe blood pressure measurement for vascular assessment (8), and its use in smartwatches for heart rate monitoring (9). It has also been investigated as a modality with which to assess vascular age, although it is not widely used for this purpose. The photoplethysmogram (PPG) signal is influenced in two ways by vascular aging. First, the time taken for the PPG pulse wave to arrive at peripheral sites reduces with chronological age, since arterial stiffness and therefore pulse wave velocity (PWV) increase with chronological age, particularly in the central arteries such as the aorta (10). Second, the shape of the PPG pulse wave changes with chronological age (11) because it is influenced by both the speed of pulse wave propagation (12) and changes in the compliance of smaller, peripheral arteries that affect wave reflection (13). Indeed, some PPG-derived parameters have been found to correlate with age (14), providing insights into the effects of age on the vasculature. The PPG is already measured by many devices with a range of designs and potential applications (see Fig. 1): PPG-based devices come in a range of form factors (e.g., from fitness bands to earbuds); measurements can be made either in contact with the skin or remotely (e.g., by finger probe or by webcam); PPG-based devices are used in clinical settings (e.g., pulse oximeters) and in daily life (e.g., smartwatches); devices can be used for continuous measurements (e.g., wearables) and intermittent measurements (e.g., placing a finger on a smartphone's camera); and measurements can be taken at different body sites (e.g., finger, wrist, and ear), and even simultaneously at multiple sites. Consequently, the PPG is an attractive and convenient modality with which to potentially assess vascular age.

This review summarizes the state-of-the-art on assessing vascular age from the PPG. It details the technical aspects of using the PPG to assess vascular age (with sufficient detail for engineers to develop the technology further), and translational aspects (aimed at clinicians and researchers). The following topics are addressed herein: indicators of vascular age which have been assessed from the PPG (see *What Indicators of Vascular Age Have Been Assessed?*, for all readers); methods used to derive these indicators of vascular age (see *How Have Indicators of Vascular Age Been Derived?*, primarily for engineers); methods used to assess their performance (see *How Has the Performance of PPG-Derived Parameters of Vascular Age Been Assessed?*, primarily for researchers); the performance of PPG-derived parameters in comparison to reference indicators (see *How Well Do PPG-Derived Parameters of Vascular Age Perform in Comparison to Reference Indicators?*, primarily for clinicians and researchers); their repeatability and reproducibility (in *How Repeatable and Reproducible Are PPG-Derived Parameters of Vascular Age?*, primarily for clinicians and researchers); their clinical utility (in *What is the Potential Clinical Utility of PPG-Derived Parameters of Vascular Age?*, primarily for clinicians and researchers); and resources and directions for future research (in *What Resources Are Available to Researchers?* and in *Future Research Directions*, primarily for researchers). Key messages for all readers are provided at the start of each section.

METHODS

The following methods were used to conduct this "systematic search and review," using a comprehensive search process to address broad research questions (15).

Research Questions

The review was designed to address the following questions:

- What indicators of vascular age have been assessed from the PPG?
- How have indicators of vascular age been derived from the PPG?
- How has the performance of PPG-derived parameters of vascular age been assessed?
- How well do PPG-derived parameters of vascular age perform in comparison to reference indicators?
- How repeatable and reproducible are PPG-derived parameters of vascular age?
- What is the potential clinical utility of PPG-derived parameters of vascular age?
- What resources are available to researchers in this field?

Search Strategy

Potential publications were identified in two steps. First, a manual search was conducted and the results were used to design a systematic search strategy. Second, this systematic search was conducted. The manual search returned 31 articles, whose titles were mostly found to include words from two themes: *1*) the PPG signal and *2*) vascular aging. Therefore, the systematic search was designed to identify publications with at least one search term corresponding to each theme in their title. The search terms are listed in Table 1. The following five search engines were used for the systematic search: ACM Digital Library, IEEE Xplore, PubMed, Scopus, and Web of Science. Electronic searches were performed on 9 June 2020 by P.H.C. No date range was used, ensuring that no restriction was placed on the date of publication. All publications identified in either the manual search or the systematic search were screened for inclusion. Further details of the search methodology are provided in APPENDIX.

Study Selection

Publications were screened against the inclusion criteria in Table 1 using the Rayyan web application (16). Briefly, to be eligible, publications had to report a method using at least one PPG signal to assess an indicator of vascular age. Indicators of vascular age were defined using the "functional and structural" biomarkers reported by Hamczyk et al. (1), with the addition of chronological age. The full list of indicators is provided in Table 1. Blood pressure (BP) was included as it "increases during aging and is associated with cardiovascular events and mortality" (1). Chronological age was

Downloaded from journals.physiology.org/journal/ajpheart (193.219.170.065) on March 9, 2022.

Figure 1. Devices for measuring the photoplethysmogram (PPG) signal. The PPG can be measured by several clinical and consumer devices, including (clockwise from *top left*): wristbands, pulse oximeters (×2), smart rings, hearables, smartwatches (×2), webcams, and smartphones. Sources (clockwise from top): P. H. Charlton, Max Health Band ("https://commons.wikimedia.org/wiki/File:Max_Health_Band.jpg") ("https://creativecommons.org/licenses/by/4.0/" CC BY 4.0); P. H. Charlton, Wrist pulse oximeter ("https://commons.wikimedia.org/wiki/File:Wrist_pulse_oximeter.jpg") ("https://creativecommons.org/licenses/by/4.0/" CC BY 4.0); Stefan Bellini, Pulox Pulse Oximeter ("https://commons.wikimedia.org/wiki/File:Pulox_Pulse_Oximeter.JPG") ("https://creativecommons.org/publicdomain/zero/1.0/" CC0 1.0) M. Verch, https://flickr.com/photos/160866001@N07/32586534637/ ("https://creativecommons.org/licenses/by/2.0/" CC BY 2.0); S. Passler et al. (242) https://doi.org/10.3390/s19173641 ("https://creativecommons.org/licenses/by/4.0/" CC BY 4.0); GEEK KAZU, https://www.flickr.com/photos/152342724@N04/36729615770/ ("https://creativecommons.org/licenses/by/2.0/" CC BY 2.0); L. Chesser, Apple_Watch_user_(Unsplash) ("https://commons.wikimedia.org/wiki/File:Apple_Watch_user_(Unsplash).jpg") "https://creativecommons.org/publicdomain/zero/1.0/" CC0 1.0); Peter H. Charlton, Webcam on computer screen ("https://commons.wikimedia.org/wiki/File:Webcam_on_computer_screen.jpg") ("https://creativecommons.org/licenses/by/4.0/deed.en" CC BY 4.0); (centre) P-H. Chan et al. (243) https://doi.org/10.1161/JAHA.116.003428 (Creative Commons Licence).

Downloaded from journals.physiology.org/journal/ajpheart (193.219.170.065) on March 9, 2022.

Table 1. *Review methodology*

The Search Strategy Used to Identify Potential Publications from Five Search Engines	
Search Theme	**Search Terms**
PPG signal	photoplethysmogra* (*additional characters), PPG, pulse contour, volume pulse, volume wave
vascular aging	age, aging, aging, BP, decomposition analysis, elasticity, hypertension, intensity analysis, PAT, PDA, peripheral, PWV, pressure, PTT, pulse arrival time, pulse transit time, pulse wave velocity, stiffness, time difference
Inclusion Criteria for the Review	
Criterion	**Inclusion**
Method	used ≥1 PPG signal
Indicator of vascular age	one or more of: *1*) arterial stiffness; *2*) blood pressure; *3*) endothelial function; *4*) intimal thickening; *5*) atherosclerosis; *6*) calcification; *7*) chronological age
Language	English
Participants	Human
Type of publication	Journal article
Source type	a primary report of performance, clinical utility, repeatability, or reproducibility.
Text availability	full text available

BP, blood pressure; PAT, pulse arrival time; PDA, pulse decomposition analysis; PPG, photoplethysmogram; PTT, pulse transit time; PWV, pulse wave velocity.

included as it has been used as a surrogate indicator of vascular age. Screening was performed using abstracts and full texts. Conference abstracts were not included as they typically did not provide enough information to address the research questions. Screening was performed collectively by the authors.

RESULTS AND DISCUSSION

Source of Evidence

Key messages: 162 articles were included in the review, the majority of which were published since 2016.

A flow diagram is provided in Fig. 2 showing how publications were identified and screened for inclusion. A total of 1,372 publications were identified in the search. After removing duplicates, 721 publications remained. Screening excluded 559 publications leaving 162 articles for analysis (14, 17–177). Figure A1 (see APPENDIX) presents the distribution of articles according to publication year. Most articles (60%) were published in the last five years, i.e., since 2016. Four journals accounted for almost a quarter of the articles: 19 (12%) in *Physiological Measurement*, 7 (4.4%) in *IEEE Transactions on Biomedical Engineering*, and 6 (3.8%) in each of *Sensors* and *American Journal of Hypertension*.

What Indicators of Vascular Age Have Been Assessed?

Key messages.

The review identified three indicators of vascular age that have been assessed from the PPG: arterial stiffness, BP, and atherosclerosis. With increasing chronological age, arterial stiffness increases, BP rises, and atherosclerosis becomes more prevalent. Each of these impacts the arrival time of the PPG pulse wave at distal sites, and the shape of the pulse wave. Associations between PPG-derived parameters and chronological age have also been investigated. Although chronological age may be suitable for the development of techniques, it may not be suitable for their validation as it cannot distinguish between subjects of the same chronological age with different vascular ages.

The vast majority of articles focused on assessing BP, with fewer assessing arterial stiffness, and very few assessing atherosclerosis (see Table A1 in APPENDIX for the numerical results). Several articles assessed the utility (clinical utility, repeatability, or reproducibility) of PPG-derived parameters. No articles were found in which endothelial function, intimal thickening, or calcification were assessed. Some articles investigated correlations between PPG-derived parameters and chronological age, although chronological age cannot distinguish between subjects of the same chronological age with different vascular ages (see Ref. 6). Therefore, the remainder of this review focuses on the following indicators of vascular age: arterial stiffness, BP, and atherosclerosis. The clinical relevance of each indicator of vascular age, and their effects on the PPG, are now described.

Arterial stiffness.

Arterial stiffness is an independent cardiovascular risk factor and a predictor of all-cause mortality (5). Arterial stiffness increases greatly with chronological age (10), resulting in increased PWV [as PWV is linked to arterial stiffness by the Moens-Korteweg equation (178)]. Arterial stiffness impacts the PPG in two ways. First, at higher PWVs the pulse transit time (PTT) from central to distal vascular locations is shorter, so the PPG pulse wave arrives earlier at distal sites. Second, the shape of the PPG pulse wave is influenced by PWV, since it is formed from incident and reflected waves whose arrival times are in part determined by PWV. The greatest change in PWV occurs in the aorta, with aortic PWV almost doubling from ~6 m/s in young adults to 10 m/s in elderly adults (10). Consequently, PPG-based methods for assessing arterial stiffness are often designed to include the aortic pathway in PWV measurements (86) or to obtain a measurement of pulse wave shape, which is related to aortic PWV (73).

PPG-based approaches for assessing arterial stiffness could be used in both clinical and consumer settings. In the clinical setting, PPG-based devices provide an alternative approach to assess PWV with potential benefits of requiring less training to use, and being less operator dependent than existing devices. When used in consumer devices, PPG-based assessment of arterial stiffness could be used to assess cardiovascular risk in daily life and identify individuals who may be at increased risk and should be offered further cardiovascular assessment.

Blood pressure.

Elevated blood pressure (BP) is a leading risk factor for disease and mortality (179). BP rises with chronological age (180), and the vascular changes that occur with chronological age are accelerated at elevated BPs (3). At low BPs, elastin bears much of the stress in the arterial wall, whereas as BP increases the load is taken up by progressively more collagen

Downloaded from journals.physiology.org/journal/ajpheart (193.219.170.065) on March 9, 2022.

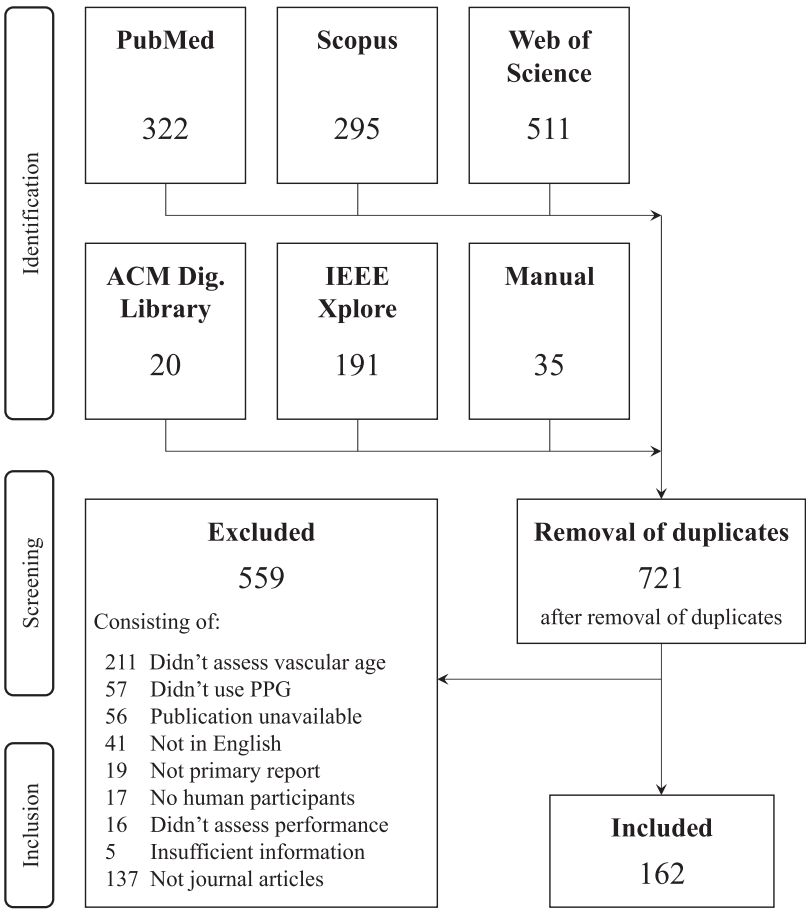

Figure 2. A summary of the identification and screening processes. PPG, photoplethysmogram.

that is much stiffer than elastin. This results in increased arterial stiffness and therefore increased PWV. Chronic increases in BP can also result in increased wall stiffness and thickness (181). The age-related change in BP varies between central (i.e., aortic) and brachial (i.e., arm) sites: the increase in central systolic BP in normal vascular aging is much greater than the increase in brachial systolic BP (182). Consequently, central BP should be preferred to brachial BP as a reference indicator of vascular age against which to compare PPG-derived indicators of vascular age. Indeed, it may be feasible to estimate a central BP waveform from a peripheral PPG waveform (141), as transfer functions have been used to relate PPG to BP waveforms at the same site (183), and to relate BP waveforms at peripheral and central sites (184). However, it may be unrealistic to use such an approach if local vascular properties impact the required transfer function, such as microvascular properties that impact the PPG.

There is potentially great benefit to assessing BP from the PPG. BP assessments could be incorporated into wearable devices such as smartwatches and fitness trackers for unobtrusive monitoring in daily life. This could help identify hypertension, and could be used to monitor BP trends such as the nocturnal dip, which has prognostic value (17). Furthermore, in the clinical setting the PPG provides an alternative approach to measure BP in peripheral locations such as the toe, by deflating a proximal cuff and identifying the appearance and disappearance of distal pulses indicating systolic and diastolic BP, respectively.

Atherosclerosis and PAD.

Atherosclerosis is a disease of the intima of the arteries, triggered by endothelial dysfunction. In more advanced cases, plaques form resulting in narrowing (arterial stenosis) of the arteries. This functional and structural pathophysiological process is a feature of vascular aging enabling its use as an indicator of vascular age (1). Atherosclerosis can reduce circulatory capability and cause end organ damage (185).

Atherosclerosis can impact the PPG in two ways. First, it has been found to be associated with increased arterial stiffness (186), with several possible mechanisms proposed linking atherosclerosis and arterial stiffness (187). Thus, atherosclerosis can result in similar changes to PPG PTT and shape as observed with increased arterial stiffness (see *Arterial stiffness*). Second, atherosclerosis can manifest in the lower limbs as PAD (155). PAD occurs when arteries carrying blood to the limbs narrow, often due to the build-up of plaque, causing a reduction in blood flow to the limbs (most often the legs). It shares common risk factors with coronary artery disease and stroke and its prevalence increases with age (188), rising from the fourth and fifth decade of life to ~15% at age 70 and over (188).

It is important to identify PAD as it is associated with increased morbidity and mortality, and yet is straightforward to treat (189). However, PAD is under-recognized and under-treated (190). PAD is typically identified through the ankle-brachial index (ABI), the ratio of systolic BP at the ankle to that at the brachial artery, with ABI $\leq$ 0.90 indicative of PAD (191). PPG-based approaches for identifying PAD could

Downloaded from journals.physiology.org/journal/ajpheart (193.219.170.065) on March 9, 2022.

potentially be automated and provide user-independent identification of PAD (23), in some cases identifying differences in PPG pulse wave shapes between limbs (106) as PAD can affect arterial function in each limb differently. Such approaches may be particularly useful for identifying PAD in primary care, with the advantages of being noninvasive and requiring minimal training (106). Although studies have demonstrated the feasibility of identifying PAD from bilateral differences in PPG pulse waves (98), it may not always be possible to differentiate between PAD and increased arterial stiffness, as they can have similar effects on the PPG.

How Have Indicators of Vascular Age Been Derived?

Key messages: Approaches to assess indicators of vascular age fall into three categories, as illustrated in Fig. 3: those which use a single PPG signal (based on pulse wave analysis), those which use multiple PPG signals (e.g., pulse transit time measurement between two PPGs), and those which use PPG and other signals (e.g., pulse arrival time measurement between the ECG and a PPG). Having used one of these approaches to derive a parameter from the PPG, a mathematical model is then often used to transform the parameter into an indicator of vascular age (such as converting pulse transit time to systolic blood pressure).

The number of articles that used each approach is now described, with results presented in Table A1. The most common approach was to use a single PPG signal (135 articles, 83%), which can be used with all PPG-based devices, including consumer devices (e.g., wristbands, smartwatches, and smartphones) and pulse oximeters. The next most commonly used approach was "PPG and other signals" (59 articles, 36%), which can be used with some advanced consumer devices [e.g., smartwatches that acquire both PPG and electrocardiogram (ECG) signals], and specialist clinical devices. The "Multiple PPG signals" approach was used least frequently (33 articles, 20%). Currently, it can only be used with specialist clinical devices.

The methods used to derive parameters from the PPG with each approach are now described, followed by a summary of how models have been used to transform PPG-derived parameters into indicators of vascular age.

Deriving parameters from a single PPG signal.

Key messages: Many methods have been proposed to derive parameters of vascular age from the PPG pulse wave, based on pulse wave analysis. These exploit the changes in pulse wave shape that occur in vascular aging. It is not yet clear which method is most suitable for assessment of vascular age.

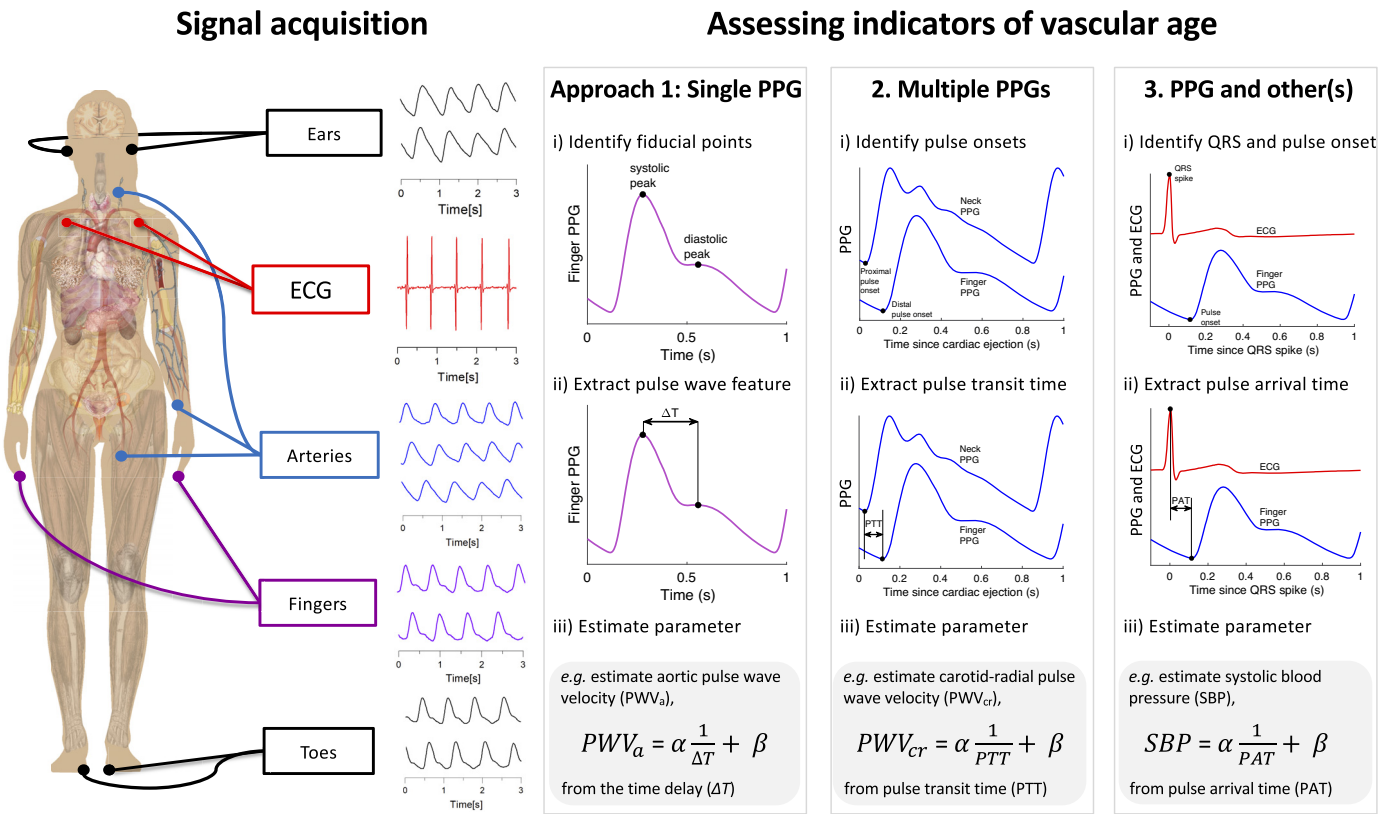

Figure 3. Three approaches for assessing indicators of vascular age from the photoplethysmogram (PPG): Signal(s) are acquired from single or multiple sites (*left*). One of three approaches is then used to derive a parameter of vascular age from the following signals: *1*) a single PPG, *2*) multiple PPGs, or *3*) PPG and other(s). An example of a regression equation for assessing an indicator of vascular age is provided for each approach: *i*) estimating aortic pulse wave velocity from the time delay between systolic and diastolic peaks on a PPG pulse wave; *ii*) estimating carotid-radial pulse wave velocity from the pulse transit time (PTT) between PPG pulse waves measured at different sites; *iii*) estimating systolic blood pressure from the pulse arrival time (PAT) between the QRS spike of an ECG signal, and the arrival of a PPG pulse wave at the finger. ECG, electrocardiogram; α and β, linear regression coefficients obtained during a calibration procedure. Sources: Mikael Häggström, Female shadow anatomy without labels ("https://commons.wikimedia.org/wiki/File:Female_shadow_anatomy_without_labels.png") (public domain); "signal acquisition" signals—Institute of Biophysics, University of Belgrade; remaining PPG signals—the Pulse Wave Database under ODC PDDL v.1.0 (https://opendatacommons.org/licenses/pddl/1-0/) (4).

AJP-Heart Circ Physiol • doi:10.1152/ajpheart.00392.2021 • www.ajpheart.org
Downloaded from journals.physiology.org/journal/ajpheart (193.219.170.065) on March 9, 2022.

Methods used to derive parameters of vascular age from a single PPG signal are based on pulse wave analysis—analysis of the shape of the pulse wave (192). Pulse wave analysis is perhaps most commonly used for the analysis of arterial BP signals, providing measures of pulse wave shape such as the augmentation index from applanation tonometry signals (193). It is already routinely used in cardiac output monitors to estimate cardiac output from the BP signal (194). The methods identified in this review to analyze a single PPG signal are summarized in Table 2.

Most of the methods quantify the shape of the PPG pulse wave, as it changes with chronological age (see Fig. 4). Pulse wave shape is influenced by both local factors [e.g., peripheral compliance (4, 167)] and systemic factors (e.g., large artery stiffness and cardiac ejection) (4, 88, 167). A dicrotic notch and a diastolic peak are visible on the downslope of *class 1* waves (see Fig. 4), which are commonly observed in young adults. These features diminish with chronological age, until they are typically no longer visible in elderly subjects (*class 4*). The pulse wave is composed of the incident wave from the heart and additional reflected

Table 2. *Methods used to derive parameters of vascular age from a single PPG signal (x)*

Pulse wave features
- Time delay: between systolic (sys) and diastolic (dia) peaks on the pulse wave (ΔT in Fig. 5B) (167).
- Stiffness index (SI): a subject's height divided by the time between sys and dia (ΔT in Fig. 5B) (73).
- Crest time (CT, also known as pulse risetime): the time from pulse onset (onset) to sys (103) (see Fig. 5B).
- Peak-to-onset time, corrected (P2Ocd): P2Ocd is the time interval between the sys and the following onset, divided by the pulse wave duration (140).
- Other time periods: including from: *1*) onset to dicrotic notch (dic) (20); *2*) sys to diastolic rise (176); *3*) sys to pulse end (176); *4*) dic to pulse end (20); *5*) diastolic rise to pulse end (176).
- Reflection index (RI): the ratio of dia and sys amplitudes (see Fig. 5B) (167).
- Augmentation index (AIx): the ratio of the amplitudes of *p2* and *p1*, defined as $[x(p2) - x(\text{onset})]/[x(p1) - x(\text{onset})]$ (88, 135).
- Dicrotic notch: the presence or absence of dic (129) (see dic in Fig. 5).
- Dicrotic notch amplitude: (79) (see dic in Fig. 5).
- Class of PPG waveform: class as determined by pulse amplitude and dic positioning (57).
- Other amplitude features: e.g., widths of individual Gaussians obtained through pulse decomposition (17).
- Statistical measures "to quantify entropy, irregularity and frequency content" of a short period of PPG (e.g., 5 s) (17, 195).
- Standardized moments of pulse wave data: skewness to quantify asymmetry, and kurtosis to quantify outliers (69).
- Shape index: the area under the pulse wave falling outside the range of healthy pulse wave shapes (98).
- Areas under the pulse wave: *1*) under the whole pulse wave (132); *2*) from onset to the maximum upslope (ms) (176); *3*) from ms to sys; *4*) from onset to sys (109); *5*) from sys to diastolic rise (176); *6*) from diastolic rise to pulse end; *7*) ratio of systolic to diastolic areas (segmented at dic in Fig. 5) (151).
- Pulse widths calculated at the height of: *1*) half the pulse wave amplitude (151); *2*) other quantiles, from 10% to 75% of the pulse wave amplitude (50, 175). Pulse widths can be divided into the width before and after sys (50).
- Compliance index: the area under the pulse wave divided by the pulse pressure (119).
- Perfusion index (PI): the ratio between the amplitudes of pulsatile and nonpulsatile components of the infrared PPG signal (119).
- Pulse amplitude (AMP): the absolute pulse amplitude, $x(\text{sys}) - x(\text{onset})$ (57), calculated from a PPG waveform which has not been normalized.
- Modified normalized pulse volume (mNPV): defined as $[x(sys) - x(\text{onset})]/x(\text{sys})$ (66), calculated from a PPG waveform which has not been normalized and retains its original offset.

First derivative features
- Slope of the rising front: the amplitude of ms, normalized by the pulse amplitude (133).
- Minimum rise time: the amplitude of the pulse wave divided by the amplitude of ms (96).
- Mean slopes: (i) between onset and sys; (ii) between sys and pulse end (151).

Second derivative features
- Fiducial point amplitudes: amplitudes of points on second derivative (*b*, *c*, *d*, and *e*), which are usually normalized by the amplitude of *a* (88) (see Fig. 5A).
- Aging index (AGI): defined as $(b - c - d - e)/a$, where *a*, *b*, *c*, *d*, and *e* are characteristic point amplitudes (88).
- Level-crossing features: the number of crossing of a contour line at a particular level on the second derivative, and the durations of the resulting segments (59).

Combinations of features
- Spring constant: defined as $x''(\text{sys})/[x(sys) - x(\text{ms})]/x(\text{sys})$ (127), derived from a physical model of the elasticity of peripheral arteries.
- Combined IPAD index: the sum of: *1*) the area under the PPG pulse wave after dic divided by the area under the pulse wave before dic, and *2*) *d*/*a* (165).
- Minimum rise time (MRT): defined as $[1/x'(\text{ms})]\cdot[x(sys) - x(\text{onset})]$ (96).
- Time intervals of periods segmented according to the polarities of the first and second derivatives (162).

Frequency domain analysis
- Normalized power of harmonics (123).
- Frequency domain features (81, 196).
- Fast Fourier Transform analysis: Use of fast Fourier transform to extract amplitude and phase information from the PPG signal (150).
- Harmonic phase shift: the phase shift between the fundamental frequency and the first-harmonic (154).
- Instantaneous frequencies: extracted using the Hilbert–Huang transform (160).
- Frequency spectrum metrics: Summary measures of the frequency spectrum, including the amplitudes and frequencies of the highest peaks, energy, and entropy (41, 69).
- Spectral power in low (LF, 0.04–0.15 Hz) and high frequency (HF, 0.15–0.40 Hz) bands, and the LF/HF ratio (81).
- Very low frequency fluctuations: pulse amplitudes or baselines are low-pass filtered to leave fluctuations which occur over 30–80 beats (29).

Features from multiple beats
- Pulse rate variability parameters (17, 32).

PPG, photoplethysmogram.

Downloaded from journals.physiology.org/journal/ajpheart (193.219.170.065) on March 9, 2022.

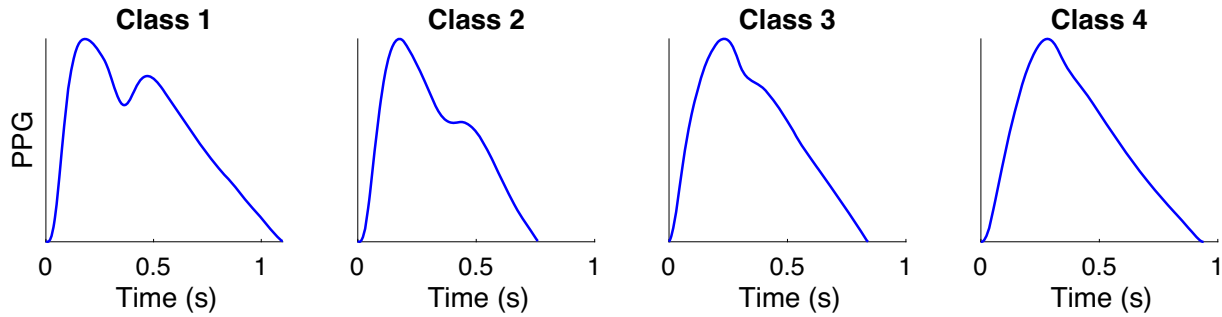

Figure 4. Classes of photoplethysmogram (PPG) pulse wave shape: Typical changes in PPG pulse wave shape with age, from young (*left*) to old (*right*). As described by Dawber et al. (244): *class 1* waves exhibit an incisura; *class 2* show a horizontal on the line of descent; *class 3* show a change in gradient on the downslope; *class 4* shows no evidence of a notch. Pulse waves were measured using infrared reflection mode photoplethysmography, and were obtained from the Vortal dataset (245). Source: P. H. Charlton, "Classes of photoplethysmogram (PPG) pulse wave shape (https://commons.wikimedia.org/wiki/File:Classes_of_photoplethysmogram_(PPG)_pulse_wave_shape.svg)" (CC BY 4.0).

waves. The speed of pulse wave propagation influences the timing of these waves, and therefore contributes to the dicrotic notch and diastolic peak characteristics (167). Consequently, vascular age has been commonly assessed from the shape of pulse waves using time- or frequency-domain (197) analysis.

Several parameters have been proposed to quantify wave shape, as illustrated in Fig. 5. When using time-domain analysis, these parameters are typically extracted by *1*) identifying fiducial points on PPG pulse waves and their derivatives (Fig. 5*A*) and *2*) calculating features (Fig. 5*B*) from the fiducial points. The features can be calculated from the timings and amplitudes of fiducial points (which can be normalized by pulse wave duration and amplitude), as well as slopes, areas, quadratic areas, and ratios of features (21, 69). Many features have been related to cardiovascular properties.

Several features have been extracted from the original pulse wave (Fig. 5*B*, *top*). The stiffness index (SI) and reflection index (RI) are commonly used, and both are influenced by the vascular state and cardiac ejection. The SI and RI are calculated from the timings and amplitudes, respectively, of the systolic (sys) and diastolic (dia) peaks on pulse waves (see Fig. 5*A*). These originate from an incident wave from the heart, followed by a temporarily spread reflected wave (assumed to consist of a number of reflected waves from around the circulation). The time delay between peaks (from which SI is calculated) is about four times the aortic pulse transit time (PTT), and is correlated with it (r = 0.75) (167). This relation is in line with reflections from the lower limbs (167). The RI (calculated from the relative amplitude of the peaks) has been found to be associated with acute changes in the stiffness of systemic arteries (167). Characteristics of the incident wave are also related to vascular aging (83), such as: the time of sys (CT), the slope of the rising front (ms), and a surrogate augmentation index (AIx). AIx is related to arterial stiffness and wave reflections. It is typically derived from the ascending aortic pressure waveform and calculated as augmentation pressure (the pressure difference between the first and second systolic peaks, *p1* and *p2*) divided by pulse pressure (198). The surrogate AIx calculated from the PPG pulse wave significantly correlates with augmentation indices calculated from radial BP pulse waves (r = 0.77) (135) and central BP pulse waves (r = 0.78 and 0.86) (88, 135). Although there are differences in the AIx derived from PPG and BP pulse waves, it has been observed that augmentation is usually positive (i.e., $p2 > p1$) on the PPG pulse wave when it is positive in the BP pulse wave, and vice-versa (135). Several methods have been used to locate *p1* and *p2* on the pulse wave, including using the second (135), third (Fig. 5*A*), and fourth derivatives (199).

Several features have been extracted from the second derivative of the pulse wave (third panel down on Fig. 5*B*) (88, 165). Five distinct peaks and troughs can be identified: *a*, *b*, *c*, *d*, and *e*. The amplitudes of *b* to *e*, normalized by that of *a*, are typically used as parameters of vascular age. The parameters *b/a*, *c/a*, and *d/a* primarily describe changes in the systolic part of the pulse wave, since points *a* to *d* occur in systole.

Each of these methods requires an algorithm to identify fiducial points, which requires careful design, particularly as pulse wave shape varies greatly with age (see Fig. 4). In the case of younger subjects, the diastolic wave peak can be detected using the second zero crossing of the first derivative of the PPG. However, pulse waves from older subjects often do not contain a distinct diastolic peak, in which case the wave location can be identified from derivatives (90, 137). The interested reader is referred to Ref. 69 for details of dicrotic notch detection (dic in Fig. 5), and Ref. 200 for details of pulse decomposition methods to identify systolic and diastolic pulse waves. Differentiation amplifies higher frequency components of a signal, so noise should be filtered out before differentiation (90). It should be noted that arterial stenosis can result in much weaker or even complete disappearance of PPG pulses (201), affecting analyses of pulse wave shape.

Frequency domain analysis has also been used to extract features from the PPG pulse wave. The fast Fourier transform is used to describe the pulse wave, with most information contained in approximately the first 10 harmonic components (or below ≈10 Hz) (123). The fundamental frequency component corresponds to the heart rate, with higher frequency harmonics at multiples of the fundamental frequency. The magnitudes of the higher frequency components are typically normalized by the magnitude of the fundamental frequency component. The magnitudes of the normalized frequency components have been found to decrease in vascular aging (96, 123).

Downloaded from journals.physiology.org/journal/ajpheart (193.219.170.065) on March 9, 2022.

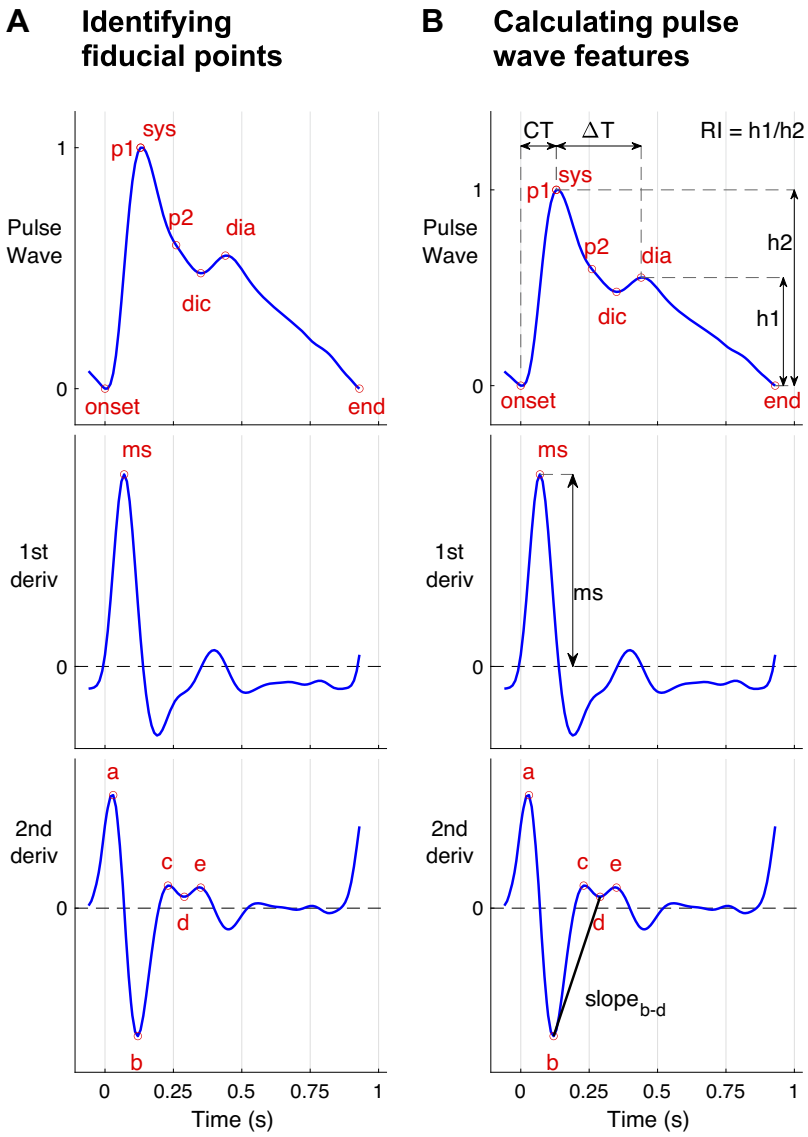

Figure 5. Extracting features from photoplethysmogram (PPG) pulse waves. Features can be extracted from a single PPG pulse wave in two steps: *A*) identifying fiducial points on the pulse wave, such as systolic (sys) and diastolic (dia) peaks, dicrotic notch (dic), early and late systolic peaks (*p1* and *p2*), the slope of the rising front (ms), and *a*, *c*, *e* peaks and *b* and *d* troughs of the 2nd derivative; and *B*) calculating features from the amplitudes and timings of these points, such as the time from pulse onset to sys (CT), the time from sys to dia (ΔT), the reflection index (RI), the maximum upslope (ms), and the slope between *b* and *d* troughs ($slope_{b-d}$). Sources: *A*: P.H. Charlton, "Photoplethysmogram (PPG) pulse wave fiducial points" (https://commons.wikimedia.org/wiki/File:Photoplethysmogram_(PPG)_pulse_wave_fiducial_points.svg) (CC BY 4.0); *B*: P.H. Charlton, "Photoplethysmogram (PPG) pulse wave indices (https://commons.wikimedia.org/wiki/File:Photoplethysmogram_(PPG)_pulse_wave_indices.svg)" (CC BY 4.0).

It is not yet clear which measures of pulse wave shape provide the best assessment of vascular age. Key technical considerations include: the physiological determinants of each feature (see Ref. 4 for examples); the reliability of pulse wave analysis algorithms for extracting features, particularly in older subjects; the site used for PPG measurement [since the pulse wave shape differs with measurement site (202)]. It would be beneficial to conduct a systematic study of different features of pulse wave shape, assessing their associations with reference indicators of vascular age, and assessing their clinical utility.

Deriving parameters from multiple PPG signals.

Key messages: Methods to assess vascular age from multiple PPG signals include *1*) measuring PTT, from which PWV can be calculated and *2*) comparison of pulse wave features between contralateral (opposite) limbs to identify PAD.

The methods used to derive parameters of vascular age from multiple PPG signals are summarized in Table 3. Most methods use two or more of the PPG measurement sites shown in Fig. 3 to acquire multiple PPG signals.

Methods using multiple PPG signals mostly assess PTT, the time delay between PPG pulse waves at two sites. PTT can be derived from two PPG signals measured from *1*) two distinct sites (e.g., finger and toe sites); *2*) two positions along an artery (e.g., lower and upper neck providing two measurements along the carotid artery); or *3*) a single site using two different wavelengths of PPG, which penetrate to different depths (indicating the time delay between pulse waves at different levels of the vasculature). There is a dichotomy between using distal sites for PTT measurement, which result in a longer PTT making it easier to measure differences in PTT (203), and using more central sites to ensure the PTT is more strongly influenced by the aorta (204). PTT can be used directly to assess vascular age, with lower values indicating a higher vascular age (87). It can also be used in conjunction with an arterial path length measurement to estimate PWV (94), allowing comparison with reference values and between subjects (10). Several body sites have been considered for PPG-based PWV measurements, including: carotid-radial, carotid-femoral, and femoral-ankle paths

Downloaded from journals.physiology.org/journal/ajpheart (193.219.170.065) on March 9, 2022.

Table 3. *Methods used to derive parameters of vascular age from multiple PPG signals*

Pulse transit time (PTT) and Pulse wave velocity (PWV)
• Multisite PTT: the delay between PPG pulse waves measured at two sites, e.g., carotid-radial, carotid-femoral, femoral-ankle (89), ear-finger, ear-toe, finger-toe (24, 87, 94).
• Single-site, dual-sensor PTT: the delay between PPG pulse waves measured using two sensors a short distance apart [e.g., proximal and distal locations along the carotid artery (170)].
• Single-site, single-sensor PTT: the delay between PPG pulse waves obtained using different wavelengths of light at a single site, e.g., the delay between infrared and blue PPGs is indicative of arteriolar PTT (the time taken for pulse waves to propagate from the arteries to the capillaries) since the infrared and blue PPGs are indicative of the arterial and capillary pulses, respectively (53).
• Estimating a parameter from PTT and pulse wave features: PTT measured between PPG signals at multiple sites, and pulse wave features, were used as inputs to a model to estimate blood pressure (61).
• PWV: calculated from PTT and the arterial path length between measurement sites (PWV = path length / PTT).
Multisite assessment of pulse wave features
• Crest time (CT, a.k.a pulse risetime) is assessed at a toe on each foot. Peripheral arterial disease is identified if the CT at either toe exceeds a threshold (62).
Multisite comparison of pulse waves
• Multisite pulse wave feature comparison: bilateral comparison of PPG pulse wave features (such as timing, amplitude or shape characteristics) between limbs (106).
• Multisite pulse wave feature comparison under hyperemia: bilateral comparison of pulse wave features (such as amplitude) between limbs: one limb exposed to hyperemia through prolonged pressure cuff inflation, and the other acting as a control (118).
• Bilateral differences: assessing bilateral blood pressure differences between index fingers to assess risk of arteriosclerosis (159).

PPG, photoplethysmogram.

(89). Different algorithms have been used to extract the timing of pulse waves, and can have a large influence on the results. For instance, the use of the "maximum of second derivative" algorithm has been found to produce finger-toe PTT measurements that correlate most strongly with carotid-femoral PTT measurements (161). This algorithm uses the *a* point on the second derivative as the marker of pulse wave timing, shown in Fig. 5*A*.

Multisite photoplethysmography (MPPG) can be used in a number of ways to detect PAD. With the expectation of bilateral similarity in PPG features for healthy subjects (similarity between opposite limbs) (205), MPPG can measure the relative delays in pulse arrival time (and/or features of normalized pulse shape) between contralateral body sides (e.g., between the great toes). Significant differences can indicate the likely presence of PAD (106), as PAD is often asymmetric in nature (due to differing locations and severities of atherosclerosis). MPPG technology can also speed up assessments by studying multiple peripheral sites simultaneously, rather than taking measurements sequentially at each site. This has the benefit that PAD can be detected even if only the pulse wave features at one limb meet the criteria for diagnosis.

MPPG has also been used to assess PWVs at several sites across the body, including the ears, fingers, and toes. However, care is needed when measuring the PWV as it can be inaccurate when significant PAD (or plaque) is present in a limb. For instance, arterial stenosis of the leg has been found to increase PTT through the leg by 20–80 ms (201), which is comparable with normal PTT measurements (such as finger-toe PTTs of 30–100 ms). If the PAD is isolated to one limb then the contralateral side could be used instead for PWV measurement (206).

Deriving parameters from the PPG and other signals.

Key messages: Methods to assess vascular age from a PPG signal and another signal include *1*) measuring pulse arrival time (PAT), *2*) measuring PTT, and *3*) using a PPG sensor and a pressure cuff to assess BP.

These methods are detailed in Table 4, and now described in turn.

PTT can be measured from the time delay between ventricular ejection and subsequent arrival of a PPG pulse wave at distal location. The time of ventricular ejection (corresponding to the pulse wave leaving the heart) can be obtained from ballistocardiography (65), seismocardiography (30), continuous wave radar (42), phonocardiography (68), or impedance cardiography (120) signals, or noncontact signals obtained using imaging PPG (164) or microwave sensors (209).

PAT is the time delay between the R-wave of the ECG and PPG pulse wave arrival, which includes not only the PTT from the heart to the PPG measurement site, but also the pre-ejection period (PEP, the time between ventricular depolarization and ventricular ejection). Consequently, while PAT decreases with chronological age due to its relationship with PTT (12), it cannot be considered a direct surrogate for PTT (210). Changes in segmental PAT (the difference between PATs at different sites) may be indicative of changes in arterial distensibility (102). PAT can be used to derive a surrogate for PWV, by using a measure of the path length along which the pulse wave travels [which can be estimated from height (114)] (91).

PTT can be estimated by measuring PEP and PAT separately, and then subtracting PEP from PAT (42, 120). This approach can be used to obtain PTT measurements when it is difficult to measure PTT directly. It accounts for inter- and intra-subject variability in PEP, providing potential improvement over using PAT alone. PEP can be estimated as the time delay between the R-wave of the ECG and a time of aortic valve opening obtained from any of: the *B* peak of an impedance cardiography signal (120); or the *I* peak of the ballistocardiogram signal (65); or the maxima of the seismocardiogram (30); or the *S1* sound in phonocardiogram (68); or by using noncontact sensors based on video or microwaves (211, 212). This approach allows PTT measurements to be obtained from devices in contact with a single point on the body [such as weighing scales (65) and wearable chest sensors (30, 68)], and from noncontact cameras (212). Consequently, the approach has potential advantages over devices that measure PTT from pulse waves at two locations, allowing measurements to be taken in daily

Downloaded from journals.physiology.org/journal/ajpheart (193.219.170.065) on March 9, 2022.

Table 4. *Methods used to derive parameters of vascular age from a PPG signal and another simultaneous signal*

Pulse arrival time (PAT)
• PAT: calculated as the delay between the R-wave in the electrocardiogram (ECG) signal and arrival of a peripheral PPG pulse wave (207).
• Segmental PAT: the difference between PAT values at different body sites such as finger and ear, or toe and ear (24).
• PAT variability: beat-to-beat PAT variability (23).
Pulse transit time (PTT)
• PTT: the delay between two pulse waves, typically one indicating ejection from the heart (e.g., using impedance cardiography), and a PPG pulse wave measured peripherally (207).
• PTT calculated from PAT and pre-ejection period (PEP): the difference between PAT and PEP, i.e., PTT = PAT - PEP (120).
Pulse wave velocity (PWV)
• PAT-derived PWV: a surrogate for PWV, calculated from PAT and a measure of arterial path length (112).
Using PPG and blood pressure (BP) measurements to assess peripheral compliance
• Peripheral compliance index: the ratio of PPG pulse amplitude to BP pulse amplitude (at finger (145) or arm (119)).
Using PPG and other signals to measure BP and ankle-brachial index (ABI)
• Volume-clamp BP measurement: A servo-controlled, inflatable finger cuff maintains a constant arterial diameter by continuously adjusting its pressure to be equal to the arterial pressure, based on a PPG measurement (156, 208).
• Identifying SBP using proximal cuff deflation: A pressure cuff is placed upstream of the PPG measurement site (arm (97), ankle (95) or toe (93, 124)), and inflated above SBP. The reappearance of a PPG pulse wave upon deflation indicates SBP. A second PPG measurement on the opposite limb can be used to reduce noise (111).
• Ankle-brachial index (ABI): systolic BP (SBP) at the ankle (identified using proximal cuff deflation) divided by SBP at the arm (measured using a sphygmomanometer) (95).

life (e.g., scales or camera) and devices to be miniaturized (e.g., chest sensor).

The PPG can be used alongside a pressure cuff to assess several parameters. First, the peripheral compliance index, which decreases with chronological age (145), can be estimated from pulse pressure and PPG pulse wave amplitude (119, 145, 171). Second, the volume-clamp method can be used to measure BP continuously (156, 208). This approach is used by several commercially available devices (213). Third, systolic BP (SBP) can be identified upon deflating a cuff proximal to a PPG probe (97) [and can be combined with Korotkoff sound measurements to increase accuracy (80)]. Finally, the ABI can be calculated from a routine brachial SBP measurement, and an ankle SBP measurement obtained using a cuff and PPG probe (95, 113).

The use of a PPG signal and another signal has the advantage that the signals can often be acquired at a single site, and there are several potential sites and measurement devices. Potential sites include measuring signals at: the ear (30), face (209), neck (52), arm (97), wrist (52), finger (145), chest (68), ankle (95), foot (65), and toe (87). In addition, several types of device have been used, including: eye glasses (214), weighing scales (65), and video cameras (209, 212).

Using models to assess indicators of vascular age from PPG-derived parameters.

Key messages: Mathematical models can be used to transform PPG-derived parameters into indicators of vascular age. Several types of model have been used, including *1*) biophysical models, based on laws of cardiovascular mechanics; *2*) statistical models, such as regression analysis; and *3*) machine learning (ML) and deep learning (DL) models.

The models identified in this review are summarized in Table 5, and are described.

Biophysical models use laws of cardiovascular mechanics to model the relationship between a PPG-derived parameter (commonly PTT or PAT) and an indicator of vascular age (such as BP). Such models have the advantage of being based on known physiological relationships, such as the link between arterial stiffness and BP, or the Windkessel model of blood flow.

Statistical models, such as regression analysis, have been used to estimate BP from PPG-derived features. Different models may be required for different use cases. For instance, different models may be required to estimate BPs from different anatomical sites [e.g., finger and wrist (202)], and to estimate systolic or diastolic BPs (69). Statistical models have the advantage that the relationships encoded in them are learnt from data.

As in many other fields, machine learning and deep learning (ML and DL) models have also received much attention for assessing vascular age (40, 70). They have been mostly used to estimate BP, or to classify subjects into diagnostic categories such as normo-, prehyper-, and hypertension. ML and DL models have the advantage that not only can they take PPG-derived parameters as inputs, but they can also take the PPG pulse wave, its spectrum or its derivative, directly as an input (75), as well as demographic information (18, 69). This avoids the need for feature extraction. DL models can capture highly complex relationships observed in training data, but have the disadvantages that they can require substantial computing resources, and are often not interpretable. A challenge in the development of ML models is to avoid "overfitting"—the development of a model that is highly specific to the training data set, and not generalizable to external data sets. To address this, feature selection algorithms have been used to reduce an initial set of features to the most valuable ones, using algorithms such as the Relief feature selection algorithm (69, 176), analysis of relevance and redundancy (21), or nonlinear mapping.

An important aspect of model development is the manner in which data are used to train, validate, and independently test a model. Cross validation allows a single data set to be used for both model training and validation, which is convenient for initial development (18, 35, 66, 77). However, to obtain reliable results, data sets should ideally be divided into training, validation, and testing sets (70), and models should be tested on external data sets. Several articles have used subject-specific model training to improve performance (41, 64, 70), which may become increasingly feasible with the widespread use of PPG-based wearables, allowing a

Downloaded from journals.physiology.org/journal/ajpheart (193.219.170.065) on March 9, 2022.

Table 5. *Models used to assess indicators of vascular age from PPG-derived parameters*

Biophysical models
- Biophysical models: mostly use the Moens–Korteweg or Hughes equations to relate the vessel wall elastic modulus to PWV and distending pressure, respectively (208), to estimate systolic (SBP), diastolic (DBP) and pulse pressure (PP) from PPG-derived parameters. Regression models are used to estimate BPs from PAT or PTT (163) (e.g., linear, logarithmic, inverse square, or inverse).
- Models can account for additional factors: such as the pulsatile change in blood vessel diameter (estimated as PPG intensity ratio) (146), and the viscous effects of blood flow (55).
- Windkessel modeling: use of a Windkessel model to assess arterial compliance (103).

Statistical models
- Auto-regressive models: (with exogenous input—ARX, and moving-average—ARMA) have been used to estimate the central BP waveform (141) and arterial SBP and DBP (174) from a PPG signal.
- Estimating measures of vascular age: various regression models (e.g., linear, inverse, quadratic, exponential, partial least-squares) are used to estimate BPs from single PPG features (44, 59, 67, 79).

Machine learning (ML) models: estimation
- Estimating measures of vascular age from a single PPG pulse wave: the pulse wave, its first and second derivatives are used as inputs to a ML algorithm [e.g., nonlinear regression (39), deep neural network (41), support vector machine (SVM) (46)] to estimate numerical values (e.g., BPs).
- Estimating measures of vascular age from pulse wave features: features are used as inputs to a ML algorithm [e.g., AdaBoost (66), random forest (35), artificial neural network (ANN) (150), regression tree (175)] to estimate numerical values (e.g., BPs).
- Estimating measures of vascular age from multiple PPGs: features derived from multisite PPGs are used as inputs to ML algorithms (e.g., SVM) to estimate numerical values [e.g., SBP, DBP (61), and ABI (76)].
- Estimating measures of vascular age from PPG and other signals: PAT and other time and complexity features from the electrocardiogram and PPG, and PPG-derived features, are used as inputs to a ML algorithm (e.g., regularized linear regression, multiadaptive regression, back-propagation error neural network, convolutional neural network (CNN), SVM) to estimate numeric values, e.g., arterial DBP and SBP (31, 34, 45, 54, 67, 72). Associations with chronological age have also been assessed (47).
- Estimating measures of vascular age from PPG and demographics: use of time-, frequency-domain and statistical features of PPGs along with demographic data as an input to a ML algorithm (e.g., ensemble trees, Gaussian process regression, multiple linear regression) to estimate numeric values, e.g., SBP and DBP (18, 69).

Machine learning (ML) models: classification
- Classifying pulse waves: use of a ML algorithm [e.g., K-nearest neighbor (KNN), CNN] to classify a pulse wave or a PPG signal transformation into a diagnostic category, e.g., normo-, prehyper- and hyper-tension (28, 74).
- Classifying sets of pulse wave features: use of a ML algorithm [e.g., SVM, ANN, decision trees or KNN] to classify a set of pulse wave features into a diagnostic category, e.g., low or high PWV (105), normal or abnormal BP (56), normo-, prehyper- and hyper-tension (21, 75).
- Classifying and then estimating measures of vascular age based on category: use of two-step ML algorithms to classify PPG features into BP categories (e.g., using KNN) and then estimate numeric values (e.g., SBP and DBP estimated using regression trees optimized for each BP category) (40).

Machine learning (ML) models: miscellaneous
- Extracting features and estimating measures of vascular age from single PPG: use of ML algorithm (e.g., CNN) to extract morphological features from a PPG segment (64) or its spectrogram (70) to estimate numerical values (e.g., BPs).
- Improving the assessment of vascular aging: use of long short-term memory networks to capture temporal dependencies between PPG features (e.g., extracted by CNN) to better track changes in measures of vascular aging (e.g., BP) (17, 64, 77).
- Reducing the feature vector: use of a ML algorithm (e.g., ANN) to nonlinearly map PPG features to reduce feature vector before estimating measures of vascular age (e.g., BPs) (50).
- Reconstructing other signals: use of wavelet neural network (149) or auto-regressive model (141) to estimate BP waveform from PPG waveform.

PAT, pulse arrival time; PPG, photoplethysmogram; PTT, pulse transit time.

subject-specific model to be trained using an individual's historical data.

How Has the Performance of PPG-Derived Parameters of Vascular Age Been Assessed?

Key messages.

Studies of PPG-derived parameters of vascular age have mostly been conducted in healthy adults, with small sample sizes. Performance has been assessed against a range of reference indicators of vascular age, using several different statistical techniques.

The characteristics of the subjects in studies of PPG-derived parameters of vascular age are summarized in Table A2, and are described. Most studies included <100 subjects, indicative of proof-of-concept studies. Most studies included young and middle-aged adults. Few studies were conducted in children, who may well benefit from vascular age assessment (215). The sex of subjects was more frequently skewed toward males than females. Most studies included apparently healthy subjects, whereas few included subjects with diabetes or PAD. Few studies have been conducted on population cohorts, which will be important to investigate the potential utility of widespread vascular age assessment.

Key aspects of the experimental methodologies used to assess PPG-derived parameters of vascular age are summarized in Table A3, and are described. Some studies used gold standard reference indicators of vascular age (e.g., invasive BP and carotid-femoral PWV), whereas others used more readily available reference indicators (e.g., noninvasive BP and PWVs acquired along alternative arterial paths). Since most clinical evidence on using BP for decision making is based on brachial cuff measurements, it is still valuable to assess BP estimates against noninvasive BPs. Chronological age was also commonly used as a surrogate indicator of vascular age. PPG-derived parameters were compared with reference indicators using statistics indicative of: correlation, agreement, error, and classification ability. Correlation measures are helpful for the development of novel indices, while the limits of agreement technique is helpful for assessing agreement between estimated and reference parameters (216) [e.g., using grand means and standard deviations to weight each subject's data equally (26)]. The performance of

Downloaded from journals.physiology.org/journal/ajpheart (193.219.170.065) on March 9, 2022.

BP estimation techniques can be compared against the Association for the Advancement of Medical Instrumentation (AAMI) and the European Society of Hypertension's (ESH) guidelines (217). Classification statistics (such as sensitivity, specificity, and *F*1-score) can be used to assess the ability of PPG-derived parameters to classify subjects into risk categories (such as hypertensive and normotensive). Most studies used a single data set, although some used multiple data sets, facilitating external validation (218). Studies using openly available data sets (see *What Resources are Available to Researchers?*) should report the subjects used in analyses to aid reproducibility.

How Well Do PPG-Derived Parameters of Vascular Age Perform in Comparison to Reference Indicators?

Key messages.

Several larger studies have compared PPG-derived parameters to reference indicators of vascular age, including comparisons of with: carotid-femoral PWV; brachial BP; and the presence of PAD.

Selected larger studies (with >40 participants) comparing PPG-derived parameters of vascular age to reference indicators are presented in Table 6.

Moderate correlations have been observed between reference PWVs (or PTTs) and those derived from PPG signals. For instance, coefficients with absolute values from 0.64 to 0.72 have been found between reference PWVs and PPG-derived parameters (finger-toe PWV and pulse wave parameters) (73, 86, 94, 127, 139). High correlations of 0.77 and 0.90 were found between reference PTTs and PPG-derived finger-toe PTT, with finger-toe PTT slightly overestimating carotid-femoral PTT by 10.6 and 17.5 ms (86, 161). Differences between PPG-based finger-toe measurements, and applanation tonometry-based carotid-femoral measurements, include: the finger-toe pathway including more peripheral vasculature; and the PPG pulse wave having a different morphology to pressure pulse waves, potentially impacting timing measurements. Moderate correlation coefficients of −0.52 and −0.67 were found between PPG-based finger-toe PTT as well as toe PAT and SBP (but not DBP) (87).

Studies have demonstrated the difficulty of estimating BP precisely from pulse wave features. BP estimates obtained from pulse wave features using ML algorithms can exhibit low bias (smaller than 0.68 mmHg), although achieving a low enough SD error of ≤8 mmHg (as required by AAMI standards) remains a challenge (35, 66). The required level of precision has been achieved by using a two-step algorithm in which pulse waves are categorized as hypo-, normo-, or hypertensive, and then BP is estimated using a model specifically for that category (40). Accurate classification into normo-, prehyper-, and hypertension BP categories has been achieved using PPG scalograms as inputs to a convolutional neural network (28). The performance of commercially available devices for continuous, noninvasive BP monitoring using the volume-clamp method was reported in a recent meta-analysis: substantial differences were found between BP estimates and reference invasive measurements, with population limits of agreement for SBP of −36 to 28 mmHg (213).

Varying strengths of correlation have been reported between indices of pulse wave shape and chronological age. The "aging index," calculated from points on the second derivative of the pulse wave (as detailed in Table 2), has been found to be highly correlated with chronological age (r = 0.80) (88). A later study confirmed this relationship although the observed correlation was lower (r = 0.42) (14).

PPG parameters have been found to be useful in detecting atherosclerotic disease, particularly PAD. Parameters obtained at the toe, such as shape index and PAT, agreed well with ABI for significant and higher-grade PAD detection with classification accuracy above 86% (106). Toe amplitude ratios as well as the aging index from the finger and the toe can discriminate between normal and abnormal ABIs (27). Also, it has been proposed that PPG probes could replace conventional Doppler ultrasound probes in ABI measurement since the two methods correlated well (r = 0.89) and PPG-based ABI had only a small bias of 0.05 (95).

How Repeatable and Reproducible Are PPG-Derived Parameters of Vascular Age?

Key messages.

PPG-derived PWVs have been found to have high repeatability and reasonable reproducibility, as have those parameters of pulse wave shape that are thought to be indicative of large artery stiffness.

The repeatability and reproducibility of PPG-derived parameters of vascular age are important aspects of their potential utility. Repeatability "refers to the variation in repeat measurements made on the same subject under identical conditions" (219), such as repeated measurements taken from a subject in a short period of time using the same device (usually within minutes while the subject is at rest). On the other hand, reproducibility "refers to the variation in measurements made on a subject under changing conditions" (219), such as measurements made by different device operators, or over an extended period of time such as days or weeks. A summary of studies reporting the repeatability or reproducibility of PPG-derived parameters of vascular age is presented in Table 7.

Some PPG-derived parameters were found to be more stable than others, even when assessed over longer periods of time. For example, PPG-derived PWV seems to be most stable, as its short-term coefficient of variation (CV) is ∼5%, and some studies report relatively good reproducibility in the longer term (121). Toe and ankle SBPs had acceptable CVs (≤6%) even when measured 3 mo apart (155).

Parameters derived from the PPG pulse wave show similar or higher variability than PWV, with a marked difference between parameters. Parameters that are indicative of large artery stiffness (e.g., stiffness index, b/a, augmentation index) were more repeatable than parameters that are strongly influenced by the smaller arteries (91, 139). Most second derivative parameters (e.g., d/a and e/a) also seemed to be less repeatable. These parameters could be more sensitive to motion artifact and small changes to the input signal.

It can be difficult to assess the repeatability of PPG-derived parameters since cardiovascular properties are ever-changing even at rest (27, 170, 220, 221). To address this, the repeatability of PPG-derived parameters has been assessed using simulated signals, which allow the performance of a device to be assessed when taking repeat measurements under identical conditions. Recently, the performance of a

Downloaded from journals.physiology.org/journal/ajpheart (193.219.170.065) on March 9, 2022.

Table 6. *Selected studies comparing PPG-derived parameters of vascular age to reference indicators*

Study	PPG Parameter	Subjects (Dataset)	Reference Indicator	Performance
Pulse wave velocity (PWV)				
Tsai et al. (94)	Finger-toe PWV	100 healthy	carotid-femoral (cf) PWV	Finger-toe PWV correlated with cfPWV ($r = 0.67$, $P < 0.01$).
Millasseau et al. (73)	Stiffness index	87 healthy	cfPWV	Stiffness index correlated with cfPWV ($r = 0.65$, $P < 0.0001$).
von Wowern et al. (139)	Aging index (AGI)	112 pregnant and nonpregnant	cfPWV	Heart rate-adjusted AGI correlated with cfPWV ($r = 0.64$, $P < 0.0001$).
Wei (127)	Spring constant	70 diabetic	cfPWV	Spring constant correlated with cfPWV ($r = –0.72$, $P < 0.001$).
Jang et al. (140)	Corrected peak-to-onset time (P2Ocd)	123 healthy	brachial-ankle (ba) PWV	P2Ocd correlated with baPWV ($r = –0.77$ and $r = –0.68$ for male and female, $P < 0.001$). Mean absolute percentage error was 7.53 ± 5.37% for average values, and 3.22 ± 1.47% for each cardiac cycle.
Pulse transit time (PTT)				
Obeid et al. (161)	Finger-toe PTT, finger-toe PWV	101 healthy and hypertensive	cfPTT, cfPWV	Correlation coefficient, root-mean-square error, and mean ± SD error were 0.90 ($P < 0.001$), 5.3 ms, −10.6 ± 5.5 ms between finger-toe PTT and cfPTT; and 0.87 ($P < 0.001$), 0.7 m/s, and 0.3 ± 0.8 m/s between finger-toe PWV and cfPWV.
Alivon et al. (86)	Finger-toe PTT, finger-toe PWV	86 healthy, hypertensive, and cognitively impaired	cfPTT, cfPWV	Correlation coefficient and mean ± SD error were 0.77 ($P < 0.0001$) and –17.5 ± 19.7 ms between finger-toe PTT and cfPTT; and 0.66 ($P < 0.0001$) and 0.2 ± 2.5 m/s between finger-toe PWV and cfPWV.
Systolic (SBP), diastolic (DBP) and mean (MBP) blood pressure (BP)				
Nitzan et al. (87)	Finger-toe PTT, toe PAT	44 healthy	Brachial BP	Finger-toe PTT and toe PAT correlated with SBP ($r = –0.52$, $P < 0.01$, and $r = –0.67$, $P < 0.0001$), but not with DBP.
Xing et al. (35)	19 pulse wave and 2nd derivative features	1,249 healthy and hypertensive	Brachial BP	Correlation coefficient and mean ± SD error for subjects ≤ 50 yr were: 0.86 and 0.45 ± 11.3 mmHg for SBP, and 0.83 and 0.31 ± 8.55 mmHg for DBP; and for > 50 yr: 0.79 and –0.68 ± 14.1 mmHg for SBP, and 0.81 and –0.20 ± 9.0 mmHg for DBP using a random forest algorithm.
Hasanzadeh et al. (66)	Pulse wave features	942 critically ill (Cuffless BP Estimation)	Invasive BP	Correlation coefficient, mean ± SD error, and mean absolute error were 0.78, 0.09 ± 10.38 mmHg and 8.22 mmHg for SBP, 0.75, –0.02 ± 5.53 mmHg and 4.58 mmHg for MBP, and 0.72, 0.23 ± 4.22 mmHg and 4.17 mmHg for DBP estimation using an AdaBoost algorithm.
Khalid et al. (40)	Pulse area, rise time, width at 25% amplitude	282 critically ill (MIMIC) and anesthetized (University of Queensland)	Brachial BP	Mean ± SD error were 0.07 ± 7.1 mmHg for SBP, and –0.08 ± 6.0 mmHg for DBP estimation using BP category-specific regression tree algorithms.
BP category				
Liang et al. (28)	PPG scalogram	121 critically ill (MIMIC)	Invasive BP category	F1 scores for classification as normotensive (NT), prehypertensive (PHT), and hypertensive (HT) were 0.81 (NT vs. PHT), 0.93 (NT vs. HT), and 0.83 [(NT + PHT) vs. HT] using a convolutional neural network.
Chronological age				
Takazawa et al. (88)	AGI	600 healthy and arteriosclerotic	Chronological age	AGI increased with age ($r = 0.80$, $P < 0.001$).
Hashimoto et al. (14)	AGI, b/a, d/a	848 healthy and hypertensive	Chronological age	AGI, b/a and d/a correlated with age ($r = 0.42$, $r = –0.35$, and $r = 0.37$, respectively, with $P < 0.001$).
Atherosclerosis category				
Allen et al. (106)	Toe PPG shape index, toe PAT, pulse amplitude	111 healthy and peripheral artery disease (PAD)	Ankle-brachial index (ABI)	Accuracy (κ) of significant and higher-grade disease detection using: shape index 91% (0.80) and 90% (0.65); bilateral difference in PAT to pulse foot 86% (0.71) and 90% (0.71); bilateral difference in PAT to pulse peak 86% (0.70) and 92% (0.76); pulse amplitude 66% (0.20) and 81% (0.34).

Continued

Downloaded from journals.physiology.org/journal/ajpheart (193.219.170.065) on March 9, 2022.

Table 6.— *Continued*

Study	PPG Parameter	Subjects (Dataset)	Reference Indicator	Performance
Peltokangas et al. (27)	Amplitude ratios, AGI	82 healthy and atherosclerotic	Abnormal ABI	Area under the ROC curve was 0.70 and 0.79 for finger and toe AGI, respectively, and 0.79 for the best performing toe amplitude ratio.
Jönsson et al. (95)	PPG ABI	43 healthy and PAD	Doppler ABI	PPG ABI correlated with Doppler ABI (r = 0.89). Mean ± SD error was 0.05 ± 0.12.

PPG, photoplethysmogram.

PPG pulse wave analysis system was assessed using pulse wave simulators (85). This provides a promising approach to assess device performance directly without the influence of physiological variations.

What is the Potential Clinical Utility of PPG-Derived Parameters of Vascular Age?

Key messages.

Much of the evidence for the potential clinical utility of PPG-derived parameters relates to identifying PAD, identifying diabetes, and risk prediction. Certain parameters of pulse wave shape have been found to be associated with cardiovascular risk.

The evidence is summarized in Table 8.

Several studies have investigated the potential clinical utility of PPG-based approaches for identifying PAD (23, 62, 106, 129, 155) using a range of parameters derived from toe PPG: pulse wave features, variability in PAT and pulse wave features, and systolic BP. Current evidence indicates that these approaches may be complementary to the ABI (such as providing increased sensitivity and decreased specificity) (129). Future research should establish which PPG-based approach provides the best performance, and to assess its clinical utility in comparison to the ABI, which is routinely used in clinical practice.

PPG-derived parameters may have utility for cardiovascular risk prediction. *d/a* has been found to be predictive of cardiovascular mortality independently of age, BP, and other atherosclerosis-related factors (169). The stiffness index has been found to be a causal risk factor for elevated BP (49), which in turn confers increased cardiovascular risk (179). The stiffness index has also been found to be associated with cardiovascular risk (108). Future research should compare the predictive performance of a wide range of PPG-derived parameters to establish which provides best performance independent of existing risk factors.

PPG-derived parameters may have utility for identifying diabetes, and for assessing how well it is controlled. Several PPG-derived parameters have been found to differ between subjects with diabetes and healthy subjects, potentially providing opportunity to identify early signs of diabetes, which can remain undiagnosed for several years (132). In addition, PPG-derived parameters have been found to be associated with glycated hemoglobin levels in patients with diabetes, providing opportunity to identify patients whose diabetes is less well controlled, and who are at greater risk of complications. It has been proposed that such approaches could be incorporated into smartphones for widespread use (222).

PPG-derived parameters may also have utility for identifying increased arterial stiffness or BP in pregnancy which can precede preeclampsia (36). It is important to identify preeclampsia early as it can result in maternal and fetal morbidity and mortality (223). PPG-equipped wearables such as smartwatches and fitness trackers present a potential approach for doing this. Current evidence on PPG-derived parameters is limited to complication-free pregnancies (36), and further research should investigate whether parameters change consistently before preeclampsia.

What Resources Are Available to Researchers?

Key messages.

Several openly available data sets are available that contain PPG signals. However, most are only suitable for assessing techniques which use a single PPG signal to estimate BP, or for investigating associations between PPG-derived parameters and chronological age.

This review identified six openly available data sets that have been used to assess PPG-derived parameters of vascular age, as summarized in Table A4. All the data sets contain a PPG signal and reference BP values, so are suitable for assessing techniques to estimate BP from a single PPG signal. Most data sets include subjects' chronological ages. The MIMIC and University of Queensland datasets also contain ECG signals, so may be suitable for assessing techniques that use both PPG and ECG signals (although the time delay between ECG and PPG signals in the MIMIC database is not necessarily constant, even within a particular subject) (231). The MIMIC data set also contains reference ABI measurements. The Pulse Wave Database contains simulated PPG pulse waves (4), so does not permit in vivo assessments, but can be used to assess how simulated pulse waves vary under a range of cardiovascular conditions (including changes in arterial stiffness) for subjects aged from 25 to 75. Consequently, it may be helpful for initial assessment of techniques, and also to aid the design of in vivo studies (4). Additional openly available data sets would be highly valuable for future research, ideally containing simultaneous ECG signals and PPG signals at different sites, and reference indicators of vascular age (such as PWV, BP, and PAD diagnoses).

There is relatively little code available to estimate parameters of vascular age from the PPG. Only one publication was identified for which the related code is publicly available (41). The "PulseAnalyse" tool (4, 232) may also be of use to researchers, as it *1*) identifies individual pulse waves in PPG signals, *2*) identifies fiducial points on pulse waves, and *3*) derives feature measurements suitable for assessing vascular age. In addition, "TTalgorithm" is a helpful script for extracting PTT measurements from simultaneous pulse wave signals (233). In the future, the field would benefit greatly from researchers making their analysis code publicly available,

Downloaded from journals.physiology.org/journal/ajpheart (193.219.170.065) on March 9, 2022.

Table 7. *Studies assessing the repeatability or reproducibility of PPG-derived parameters of vascular age*

Study	PPG Parameter	Subjects	Delay	Findings
Pulse wave velocity (PWV)				
Loukogeorgakis et al. (89)	PWV along: carotid-femoral, arm and leg	Healthy 10 min: 10 3 h: 5	10 min 3 h	Coefficient of variation (CV): -carotid-femoral: 5.7% (10 min), 6.3% (3 h) -arm: 5.6% (10 min), 13.0% (3 h) -leg: 4.6% (10 min), 16.1% (3 h)
Tsai et al. (94)	Finger-toe PWV	20 healthy	20 min	Intra-class correlation coefficient (ICC): 0.959 Limits of agreement: 0.09 ± 0.69 m/s CV: 5.8%
Nabeel et al. (170)	Local carotid PWV	35 healthy	Beat-to-beat 10 s	CV: from 4.15% to 11.38% (beat-to-beat) Limits of agreement: 0.02 ± 0.22 m/s (10 s) Correlation coefficient: 0.96 (10 s)
Jang et al. (140)	Brachial-ankle PWV (estimated)	HealthyIndividual: 123 Average: 47	None	CV (individual pulse waves analyzed): 2.52% CV (average from several pulse waves): 0.27%
Liu et al. (121)	Heart-ear, heartfinger, heart-toe PWV (bilateral)	15 healthy	3 mo	Technical error of measurement (TEM) and relative TEM (rTEM): -heart-ear: TEM 0.005 and 0.0058, rTEM 4.7% and 5.4% -heart-finger: TEM 0.0538 and 0.0601, rTEM 1.2% and 1.2% -heart-toe: TEM 0.054 and 0.0661, rTEM 1.1% and 1.3%
Nabeel et al. (173)	Local carotid PWV	25 healthy	10 s	Correlation coefficient: 0.97 Limits of agreement: −0.01 ± 0.19 m/s
Alivon et al. (86)	Finger-toe PWV	38 unhealthy, 7 healthy	5 min	CV: 4.52% Limits of agreement: 0.02 ± 0.98 m/s
Systolic (SBP), diastolic (DBP) and mean (MBP) blood pressure (BP)				
Scanlon et al. (124)	Toe BP, toe-brachial index (TBI)	60 patients with diabetes	7 days	ICC and standard error of measurement (SEM): -toe BP intrarater reliability: ICC 0.78–0.79, SEM 8 mmHg -toe BP interrater reliability: ICC 0.93, SEM 4 mmHg -TBI intrarater reliability: ICC 0.51–0.72, SEM 0.08 -TBI interrater reliability: ICC 0.85, SEM 0.07
Hoyer et al. (155)	Ankle and toe SBPs	60 unhealthy	3 mo	CV of toe SBP: Vicorder device 5.63%, Falcon device 6.36% CV of ankle SBP: Vicorder device 3.43%, Falcon device 4.01%
Single PPG pulse wave parameters				
von Wowern et al. (139)	Finger PPG indices	112 Healthy and unhealthy	Consecutive measurements	Good repeatability (ICC $\geq$ 0.80): aging index (AGI), dicrotic index, dicrotic dilatation index, cardiac ejection elasticity index, *b*/*a*, *e*/*a*. Moderate repeatability (ICC: 0.50–0.79): elasticity index, *c*/*a*, *d*/*a*, *a*–*b* and *a*–*e* intervals. Poor repeatability (ICC $<$ 0.50): ejection time compensated, dicrotic elasticity index, a-c and a-d intervals.
Peltokangas et al. (27)	AGI and amplitude ratios from 5 body locations	Atherosclerotic, healthy	Beat-to-beat Single session 3 days	Beat-to-beat: ICCs mostly >0.8. Single session: ICCs mostly >0.95, average intra-subject CV $<$ 0.1. 3 days: ICCs for some indices >0.6, with few >0.8.
Millasseau et al. (73)	Finger stiffness index (SI)	8 healthy	1 wk	Within-subject CV: 9.6%
Millasseau et al. (91)	Finger PPG indices	8 healthy	Short-term: same day Long-term: $\geq$ 3 days	Within-subject CV: high short-term repeatability (<5%): SI, reflection index, b/a low short-term repeatability (>10%): *c*/*a*, *d*/*a*, *e*/*a* high long-term repeatability (<10%): SI, *b*/*a* low long-term repeatability (>10%): reflection index, *c*/*a*, *d*/*a*, *e*/*a*

Continued

Downloaded from journals.physiology.org/journal/ajpheart (193.219.170.065) on March 9, 2022.

Table 7.— *Continued*

Study	PPG Parameter	Subjects	Delay	Findings
Kulin et al. (85)	Finger PPG indices	Pulse wave simulator, 10 healthy	minutes	Pulse wave simulator: very low CVs (<1%) for all parameters in "normal" mode; high CVs (>10%) for AGI, *d*/*a* and *c*–*d* detection ratio in "abnormal" mode. Healthy subjects: low CVs (<5%) for left ventricular ejection time, heart rate, interbeat interval, b/a, SI; moderate CV (7.4%) for reflection index; high CVs (>10%) for AGI, *c*–*d* detection ratio, *d*/*a*.
Gunarathne et al. (108)	Finger SI	100 healthy	5 min weeks	Limits of agreement: 0.09 ± 1.32 m/s (5 min), 0.12 ± 1.86 m/s (6 wk)
Other parameters				
Tanaka et al. (116)	Finger MBP, finger arterial SI and elasticity index	6 healthy	day(s)	Mean CV: MBP 4.51%, SI 5.72%, elasticity index 8.20%
LopezBeltran et al. (145)	Peripheral vascular compliance index	9 healthy	Single session	CV: from 11.3% to 15.1% depending on MBP

PPG, photoplethysmogram.

aiding reproducibility, and allowing others to build on their work. The Papers with code website (https://portal.paperswithcode.com/) may be helpful for this, which facilitates sharing of code and data, and has a leaderboard of techniques used to estimate BP from the PPG (see https://paperswithcode.com/task/blood-pressure-estimation).

In the future, data sets containing annotations of fiducial points on PPG pulse waves could be used to assess pulse wave analysis algorithms. We are not aware of any data sets containing manual annotations of fiducial points, although the Pulse Wave Database does contain machine-generated annotations (4).

Future Research Directions

Key messages.

There is much further work to be done to realize the full potential of PPG-based devices for assessing vascular age. Several directions have been identified in the areas of *1*) science and technology of measurements, *2*) clinical considerations and wider validation, and *3*) sensors and computing science.

This review has demonstrated the great potential of using the PPG to assess vascular age. A resurgence of interest in the PPG has been driven by: the demand for low-cost, simple, and portable technology suitable for primary care and community-based clinical settings; the availability of low-cost and miniature semiconductor components; and advances in pulse wave analysis techniques. Interest in the PPG has continued to grow with the development of: state-of-the-art wearable sensors; digital health and smartphone platforms; ML and artificial intelligence (AI) based analysis techniques; and cloud-based analytics. The Covid-19 pandemic appears to have accelerated developments in healthcare technologies, including PPG devices and their applications (234, 235). Despite such innovation, several research questions remain unanswered, as now outlined. Future research into using the PPG to assess vascular age will benefit from interdisciplinary collaboration to address these questions, often requiring consensus agreement.

Science and technology of measurements.

- *Physiological origins:* To better understand the origins of the PPG signal, since its physiological origins are still not well understood (236). The origins of both the "AC" pulse wave and the lower frequency "DC" components should be further investigated.
- *Measurement and analysis technology:* To further understand the influence of technical factors such as operating wavelength(s), probe-tissue interface pressure, sampling frequency, the mode of PPG used (reflection or transmission), and the acquisition of PPG signals by contact or noncontact ("imaging") methods.
- *Reproducibility:* To use an agreed measurement procedure that has been demonstrated to improve reproducibility in studies, including specifications such as: body position, anatomical measurement site, duration of measurement, PPG sensor configuration, and signal processing techniques. To openly share repeatability and reproducibility data in publications as standard. To gather a minimum data set that includes participant demographics and key measurement parameters used for the PPG recording.
- *Normal ranges:* To establish normal ranges for PPG-derived parameters at different body sites and across different populations, including stratification by sex, skin pigmentation, and chronological age.
- *Signal quality:* To standardize signal quality indices, and optimize the design of algorithms for PPG noise and artifact rejection. Furthermore, the potential benefits of acquiring other signals simultaneously to enhance or monitor PPG signal quality should be further investigated, such as accelerometer or gyroscope signals for noise detection and cancellation (92).
- *Understanding variability:* To understand the variability in PPG-derived parameters. To understand normal physiological variability (such as short-term variability during a measurement and diurnally) so that average "representative" measures can be extracted for analysis. To understand the influence of cardiac arrhythmias such as atrial fibrillation, and their impact on vascular

Downloaded from journals.physiology.org/journal/ajpheart (193.219.170.065) on March 9, 2022.

Table 8. *Studies on the potential clinical utility of ppg-derived parameters of vascular age*

Study	PPG Parameter	Health Status	Findings
Identifying atherosclerosis, including peripheral arterial disease (PAD)			
Bortolotto et al. (51)	Augmentation index (AIx), aging index (AGI)	Hypertensive, some atherosclerotic	The AGI may have some utility as a measure of atherosclerosis in older hypertensives, although carotid-femoral PWV had better performance.
Peltokangas et al. (27)	Amplitude ratios, AGI	Healthy and atherosclerotic	The AGI and some amplitude ratios measured at second toe may have utility as a measure of atherosclerosis (ROC AUC 0.79).
Allen et al. (106)	Toe pulse arrival time (PAT), shape index, rise time, amplitude	Healthy and PAD	All parameters differed between healthy and PAD. The bilateral differences in parameters (except normalized amplitude) differed between healthy and PAD.
Ro et al. (129)	Toe PPG pulse waves	Healthy and PAD	Identified PAD through manual review of toe pulse waves. This provided complementary performance to the ankle-brachial index (ABI).
Bentham et al. (23)	Variability in pulse amplitude and PAT	Healthy and PAD	Variability in amplitude reduced, and variability in PAT increased, in PAD.
Wu et al. (38)	PPG pulse wave timings	Healthy and diabetic	Results indicated that PPG pulse wave timings could be used to discriminate between healthy and diabetic subjects.
Risk prediction			
Kuznetsova et al. (82)	Pulse amplitude after occlusion	Population cohort	Change in pulse amplitude after occlusion correlated weakly with cardiovascular risk factors.
Inoue et al. (169)	*d/a*	Population cohort	*d/a* found to be an independent predictor of cardiovascular mortality.
Zekavat et al. (49)	Stiffness index (SI)	Population cohort	SI found to be a genetically causal risk factor for blood pressure but not coronary artery disease.
Gunarathne et al. (108)	SI	Healthy, hypertensive, diabetic, hyperlipidemic	SI was associated with cardiovascular risk (HeartScore) and able to discriminate between risk categories.
Identifying and stratifying subjects with diabetes			
Wei et al. (25)	SI, instantaneous energy of maximal energy (f_{Emax})	Healthy, diabetic	SI and f_{Emax} were higher in diabetic subjects than age-matched healthy subjects. f_{Emax} was associated with glycated hemoglobin levels (indicative of how well diabetes is controlled) and fasting blood sugar levels.
Wu et al. (159)	Pulse amplitudes, pulse wave velocity (PWV) (bilateral)	Healthy, diabetic	Bilateral differences in pulse amplitudes and PWV were sensitive to elevated glycated hemoglobin levels, and were correlated with cardiovascular risk factors.
Usman et al. (132)	Area under the pulse wave	Diabetic	The area under the pulse wave was lower in patients with higher glycated hemoglobin levels (and higher risk of complications).
Pilt et al. (90)	AGI	Healthy and diabetic	AGI higher in diabetic subjects than age-matched healthy subjects.
Pilt et al. (135)	AIx	Healthy and diabetic	AIx higher in diabetic subjects than age-matched healthy subjects.
Pilt et al. (133)	Slope of the rising front (ms)	Healthy and diabetic	The slope of the rising front can be used to discriminate between healthy and diabetic subjects.
Miscellaneous			
Wang et al. (119)	Finger-toe PWV, compliance index (CI)	Healthy and chronic kidney disease	CI and PWV differed between healthy subjects and chronic kidney disease patients, and changed with disease progression. A decrease in CI was associated with an increase in the number of cardiovascular risk factors. CI was independently associated with estimated glomerular filtration rate.
Sangle et al. (130)	SI	Healthy and patients with livedo	No difference in SI between groups despite more abnormal carotid-femoral PWV in patients with livedo.
von Wowern et al. (36)	AGI, *b/a*, *d/a*	Pregnant women	Parameters changed during pregnancy, but variance was greater than the influence of gestational age.
Bereksi-Reguig et al. (166)	AIx, *b/a*	Healthy and pathologic	Both PPG-derived parameters differed between normal and pathological subjects.
Sharkey et al. (24)	Toe-finger, toe-ear, finger-ear pulse transit time (PTT)	Children: healthy and heart transplant	PTT was increased in children who have successfully undergone cardiac transplantation.

Continued

AJP-Heart Circ Physiol • doi:10.1152/ajpheart.00392.2021 • www.ajpheart.org
Downloaded from journals.physiology.org/journal/ajpheart (193.219.170.065) on March 9, 2022.

Table 8.— *Continued*

Study	PPG Parameter	Health Status	Findings
Dillon and Hertzman (101)	Crest time (CT)	Healthy, hypertensive, and arteriosclerotic	Crest time was increased in hypertensive and arteriosclerotic patients. Changes were greater, and visible at an earlier stage of disease, in finger compared to radial PPG signals.
Tanaka et al. (116)	Finger arterial SI	Healthy, arteriosclerotic	The SI appeared to be higher in arteriosclerotic subjects.
Kiselev and Karavaev (81)	Indices of frequency spectral power	Healthy, hypertensive, coronary artery disease	High frequency power (HF%, 0.15–0.40 Hz) increased in disease; low frequency power (LF%, 0.04–0.15 Hz) and LF/HF decreased.

PPG, photoplethysmogram.

aging assessments. To understand the utility of PPG-derived parameters acquired during sleep, which are less likely to be contaminated with motion artifact (237), but may not provide the wealth of information afforded by measurements taken during activities of daily living (238).

Clinical considerations and wider validation.

- *Systematic assessment of existing parameters:* To systematically assess existing PPG-derived parameters of vascular aging (e.g., the stiffness index and those derived from the second derivative) to understand which parameters (or combinations of parameters) are most suitable for assessing vascular age.
- *Physiological determinants:* To understand further the influence of confounding factors on PPG-derived parameters, such as the influences of heart rate and BP.
- *Microcirculation:* To understand further the impact of the microcirculation on PPG-derived parameters, and determine how we might use this insight to improve assessments. Although several methods are available for assessing arterial stiffness, the PPG signal has a particular but seldom explored advantage, that it can provide composite macrovascular and microvascular information. To date, most techniques for assessing vascular age from the PPG focus on the larger blood vessels. The microcirculation may also provide useful information, and can be assessed in a multisite PPG configuration (using bilateral and ipsilateral body site comparisons) (205). Strict protocols should be employed for microvascular measurements, considering: a rest period before measurements; room temperature; and careful handling of tissue sites so as not to invoke perfusion changes. Also, the potential utility of PPG-derived measures of endothelial and autonomic function (239) should be investigated, and their associations with arterial stiffness and atherosclerosis measures.
- *Validating parameters:* To develop and clinically validate PPG-derived parameters of vascular age against a recognized gold standard for "vascular age," rather than chronological age. The ultimate goal should be to develop and validate PPG-based biomarkers of vascular age (185, 240).
- *Assessing reliability:* To assess the reliability of PPG-derived parameters of vascular age, i.e., the relative magnitude of measurement errors in comparison to true differences between subjects (219).
- *Unobtrusive monitoring in daily life:* Approaches which use a single PPG signal could be incorporated into wearables such as smartwatches, providing opportunity to assess vascular age in large numbers of subjects in daily life. Although such an approach may not provide a gold-standard assessment of vascular age, it could be complementary to the current gold standard of carotid-femoral pulse wave velocity: the sensors would be less expensive; measurements would not require a trained operator; and by taking measurements during sleep, measurements could be standardized (same time of day, and supine position), and the subject would not need to set aside time to rest before measurement. To achieve this, technologies should be robust and resilient to movement artifact and noise, incorporated into consumer devices, and ideally have applications in health and well-being. Such measurements could be incorporated into wrist-worn devices, finger probes, and weighing scales for longitudinal assessments easily made in the home (65).

Sensors and computing science.

- *Sensors:* To develop novel PPG sensors for the specific goal of assessing vascular age. This should consider also the attachment of sensor to tissue for repeatable measurements, for example to stabilize the contact by applying an external pressure (76, 78). PPG sensors should be designed to mitigate against probe-tissue signal artifacts and to help obtain high-quality signals (241). Ideally, PPG sensors should be standardized to ensure measurements are replicable.
- *Artificial intelligence:* To exploit the power of AI (including explainable AI) and potentially quantum healthcare technologies for PPG processing and to help model and understand big data sets stemming from worldwide sampling.

CONCLUSIONS

The PPG signal is emerging as a potential tool for assessing vascular age, with potential applications in clinical and consumer devices. The shape and timing of the PPG pulse wave are both influenced by normal vascular aging, changes in arterial stiffness and blood pressure, and atherosclerosis. Consequently, a plethora of approaches have been proposed to assess vascular age from the PPG. These approaches fall into three categories: *1*) those which use a single PPG signal

Downloaded from journals.physiology.org/journal/ajpheart (193.219.170.065) on March 9, 2022.

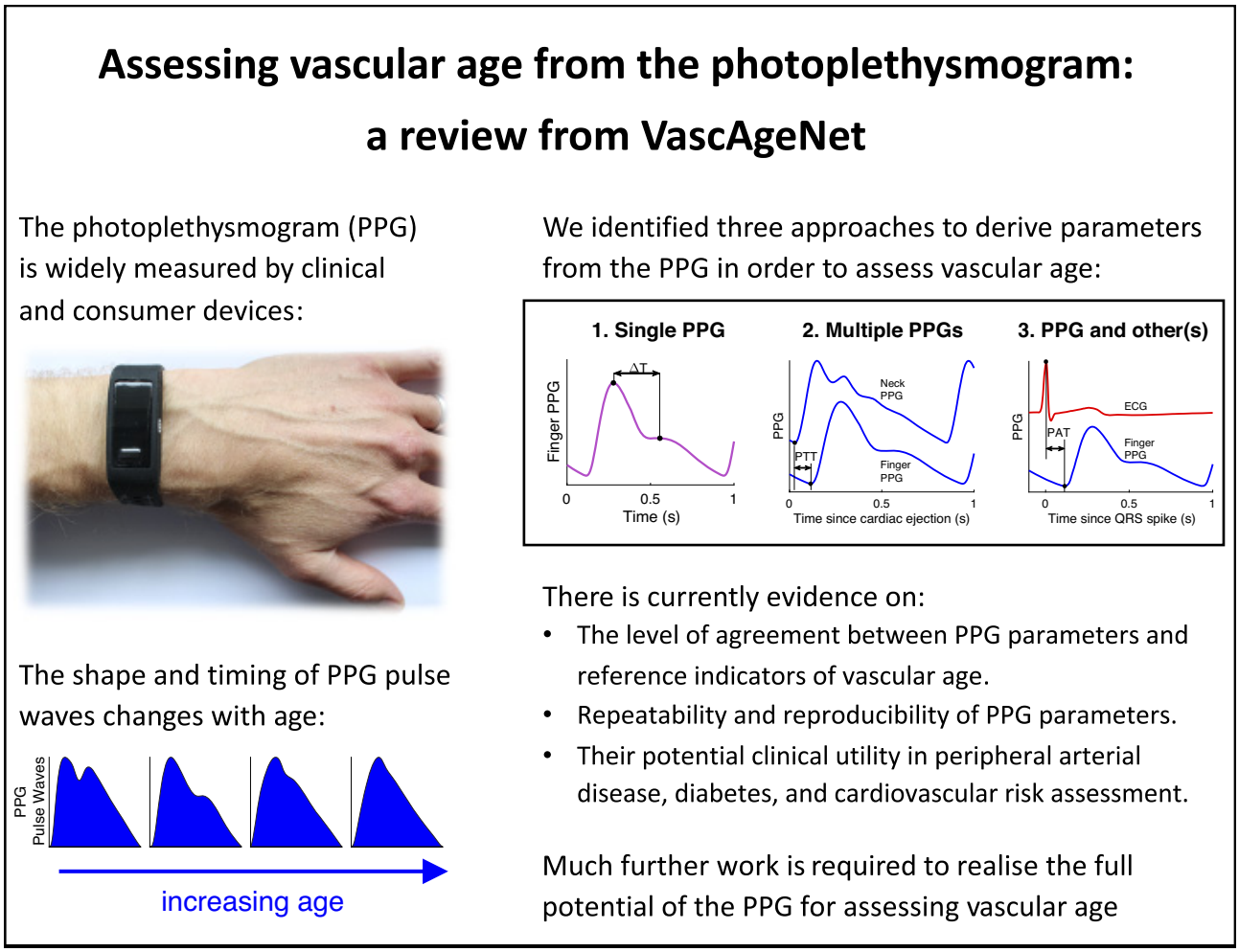

Figure 6. A graphical summary of the key conclusions. Wristband adapted from P. H. Charlton, "Max Health Band" (CC BY 4.0). Pulse waves adapted from: P. H. Charlton, "Classes of photoplethysmogram (PPG) pulse wave shape" (CC BY 4.0).

(based on pulse wave analysis), *2*) those which use multiple PPG signals (e.g., PTT measurement), and *3*) those which use PPG and other signals (e.g., PAT measurement). There is evidence in the literature on the level of agreement between PPG-derived parameters and reference indicators of vascular age, and on the repeatability and reproducibility of selected parameters. Furthermore, the clinical utility of PPG-derived parameters has been explored in the fields of PAD, diabetes, and cardiovascular risk prediction. However, there is much further work to be done to realize the full potential of PPG-based devices for assessing vascular age.

Key directions for future work include:

- Gaining a better understanding of the physiological origins of the PPG signal, and how it is influenced by the stiffness of large and small arteries.
- Standardizing measurement techniques to ensure that PPG-derived parameters are measured robustly, both for clinical decision making and in the rapidly growing consumer market.
- Validating PPG-based techniques for assessing vascular age, and assessing their potential clinical utility.

Figure 6 provides a graphical summary of these conclusions.

APPENDIX

Search Methodology

Search commands.

The search commands used with each search engine were as follows:

ACM digital library. The ACM Digital Library Advanced Search (https://dl.acm.org/search/advanced) was used to search the "ACM Guide to Computing Literature" with the following query:

Title:(photoplethysmogra OR ppg OR "pulse contour" OR "volume pulse" OR "volume wave") AND Title:(age OR ageing OR aging OR BP OR "decomposition analysis" OR elasticity OR hypertension OR "intensity analysis" OR PAT OR PDA OR peripheral OR PWV OR pressure OR PTT OR "pulse arrival time" OR "pulse transit time" OR "pulse wave velocity" OR stiffness OR "time difference")*

IEEE xplore. The IEEE Xplore "Command Search (https://ieeexplore.ieee.org/search/advanced/command)" was used to search with the following query:

(((("Document Title":photoplethysmogra) OR "Document Title":ppg) OR "Document Title":"pulse contour") OR "Document Title":"volume pulse"[Title]) OR "Document*

Downloaded from journals.physiology.org/journal/ajpheart (193.219.170.065) on March 9, 2022.

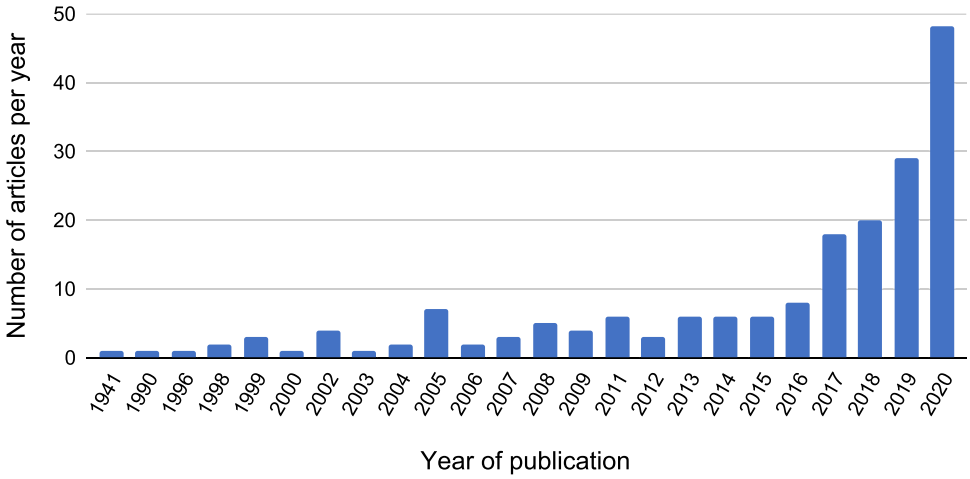

Figure A1. The number of included articles published per year.

Title":"volume wave"[Title]) AND ((((((((((((((((((("Document Title":age) OR "Document Title":ageing) OR "Document Title":aging) OR "Document Title":BP) OR "Document Title":"decomposition analysis") OR "Document Title":elasticity) OR "Document Title":hypertension) OR "Document Title":"intensity analysis") OR "Document Title":PAT) OR "Document Title":PDA) OR "Document Title":peripheral) OR "Document Title":PWV) OR "Document Title":pressure) OR "Document Title":PTT) OR "Document Title":"pulse arrival time") OR "Document Title":"pulse transit time") OR "Document Title":"pulse wave velocity") OR "Document Title":stiffness) OR "Document Title":"time difference")

PubMed. The "PubMed Advanced Search Builder (https://pubmed.ncbi.nlm.nih.gov/advanced/)" was used to search with the following query:

(((((photoplethysmogra[Title]) OR ppg[Title]) OR "pulse contour"[Title]) OR "volume pulse"[Title]) OR "volume wave"[Title]) AND ((((((((((((((((((age[Title]) OR ageing[Title]) OR aging[Title]) OR BP[Title]) OR "decomposition analysis"[Title]) OR elasticity[Title]) OR hypertension[Title]) OR "intensity analysis"[Title]) OR PAT[Title]) OR PDA[Title]) OR peripheral [Title]) OR PWV[Title]) OR pressure[Title]) OR PTT[Title]) OR "pulse arrival time"[Title]) OR "pulse transit time"[Title]) OR "pulse wave velocity"[Title]) OR stiffness[Title]) OR "time difference"[Title])*

Scopus. The Scopus "Advanced Search (https://www.scopus.com/search/form.uri?display=advanced)" was used to search with the following query:

TITLE(photoplethysmogra OR ppg OR "pulse contour" OR "volume pulse" OR "volume wave") AND TITLE(age OR ageing OR aging OR BP OR "decomposition analysis" OR elasticity OR hypertension OR "intensity analysis" OR PAT OR PDA OR peripheral OR PWV OR pressure OR PTT OR "pulse arrival time" OR "pulse transit time" OR "pulse wave velocity" OR stiffness OR "time difference") AND NOT INDEX (medline)*

Web of science. The Web of Science "Advanced Search" was used to search the "Web of Science Core Collection" with the following query:

TI=(photoplethysmogra OR ppg OR "pulse contour" OR "volume pulse" OR "volume wave") AND TI=(age OR ageing OR aging OR BP OR "decomposition analysis" OR elasticity OR hypertension OR "intensity analysis" OR PAT OR PDA OR peripheral OR PWV OR pressure OR PTT OR "pulse arrival time" OR "pulse transit time" OR "pulse wave velocity" OR stiffness OR "time difference")*

Collating search results.

Results from each search engine were downloaded as text files. Files were obtained in Bibtex format for all search engines apart from PubMed, for which the "*Abstract (text)*" format was used. The results were then collated using the *ppg_vascage_review_collate_search_data.m* MATLAB script, available in Supplemental material at https://doi.org/10.5281/zenodo.5039640.

Removing duplicates.

Duplicate publications were identified as any publications with the same DOI; any publications with the same title and other consistent details (such as authors and year of article). A few additional duplicates were identified using the Rayyan web application (16).

Table A1. *The number of articles which used each approach to assess vascular age, and which assessed each indicator of vascular age*

	Blood Pressure	Stiffness	Atherosclerosis	Chronological Age	Utility	All
Single PPG	50	15	2	17	11	135
Multiple PPG	11	3	3	1	4	33
PPG and Other(s)	41	9	2	2	7	59
All	95	26	4	20	21	

NB: Some articles used more than one approach or one indicator. PPG, photoplethysmogram.

Downloaded from journals.physiology.org/journal/ajpheart (193.219.170.065) on March 9, 2022.

Table A2. *Characteristics of participants in studies of PPG-derived parameters of vascular age*

Category	No. Articles (%)
Number of subjects	
≤9	8 (4.9)
10–49	65 (40.1)
50–99	32 (19.8)
100–499	43 (26.5)
500–999	6 (3.7)
≥1,000	7 (4.3)
Unknown	1 (0.6)
Age(s) of subjects, yr	
≤17: Pediatric	6 (3.7)
18–39: Young adult	104 (64.2)
40–69: Middle-aged adult	107 (66.0)
≥70: Elderly adult	73 (45.1)
Unknown	30 (18.5)
Proportion of subjects who were female, %	
0–20: Mostly male	22 (13.6)
21–40: Primarily male	23 (14.2)
41–60: Well balanced	46 (28.4)
61–80: Primarily female	10 (6.2)
80–100: Mostly female	6 (3.7)
Unknown	55 (33.0)
Most common health statuses	
Healthy	118 (72.8)
Unhealthy (nonspecific)	24 (14.8)
Critically ill	17 (10.5)
Hypertensive	17 (10.5)
Diabetic	15 (9.3)
Peripheral arterial disease	8 (4.9)
Population cohort	4 (2.5)
Under anesthesia	4 (2.5)

Table A3. *Methods used to assess the performance of PPG-derived parameters of vascular age*

Category	No. Articles (%)
Reference indicator of vascular age	
Blood pressure: noninvasive	60 (37.0)
Blood pressure: invasive	23 (14.2)
Chronological age (a surrogate)	20 (12.3)
Ankle-brachial index	12 (7.4)
Pulse wave velocity: carotid-femoral	11 (6.8)
Pulse wave velocity: other paths	5 (3.1)
Pulse arrival time	3 (1.9)
Pulse transit time	1 (0.6)
Other stiffness indices, e.g., AIx	6 (3.7)
None	21 (13.0)
Common statistical measures	
Correlation coefficient	75 (46.3)
Bias + limits of agreement	54 (33.3)
Mean absolute (percentage) error	23 (14.2)
Root-mean-square error (RMSE)	14 (8.6)
Classification statistics, e.g., sens, spec	20 (12.3)
Number of datasets used	
1	141 (87.0)
2	15 (9.3)
≥ 3	6 (3.7)

AIx, augmentation index.

Additional publications.
Four additional publications were added to the manual search during the course of the review (82, 83, 85, 86).

Distribution of Articles According to Publication Year

The distribution of articles according to publication year is presented in Fig. A1, and discussed in *Source of Evidence*.

Approaches Used to Assess Indicators of Vascular Age

The approaches used to assess the different indicators of vascular age are summarized in Table A1, and discussed in *What Indicators of Vascular Age Have Been Assessed?* and in *How Have Indicators of Vascular Age Been Derived?*

Methods Used to Assess the Performance of PPG-Derived Parameters of Vascular Age

The characteristics of the subjects in the included studies of PPG-derived parameters of vascular age are summarized in Table A2, and discussed in *How Has the Performance of PPG-Derived Parameters of Vascular Age Been Assessed?*

Key aspects of the experimental methodologies used to assess PPG-derived parameters of vascular age are summaries in Table A3, and discussed in *How Has the Performance of PPG-Derived Parameters of Vascular Age Been Assessed?*

Methods Used to Assess the Performance of PPG-Derived Parameters of Vascular Age

The openly available data sets that have been used to assess PPG-derived parameters of vascular age are summarized in Table A4, and discussed in *What Resources are Available to Researchers?*

GRANTS

This article is based upon work from COST ACTION "Network for Research in Vascular Ageing" CA18216 supported by COST (European Cooperation in Science and Technology): www.cost.eu. The work was supported in part by British Heart Foundation Grants PG/15/104/31913 and FS/20/20/34626 (to P. H. Charlton); in part by the European Regional Development Fund Project No. 01.2.2-LMT-K-718-01-0030 (to V. Marozas) under grant agreement with the Research Council of Lithuania; in part by the Estonian Ministry of Education and Research under personal post-doctoral research funding PUTJD815 (to K. Pilt); and in part by the Serbian Ministry of Education, Science and Technological Development Grants 32040 and 41022 (to D. Žikić).

DISCLOSURES

S. Zanelli collaborates with Axelife, a company that designs and develops PPG-based medical devices. D. Kulin is shareholder and employee in E-Med4All Europe Ltd., a Hungarian med-tech startup developing various PPG-based telemedicine solutions. M. Hallab is CEO of Axelife and has authored patents used by Axelife. E. Bianchini is co-founder of QUIPU s.r.l., Pisa, Italy, a spin-off company of the Italian National Research Council and the University of Pisa developing medical software for ultrasound image processing. V. Dittrich is CEO and shareholder of Redwave Medical GmbH, a company developing medical algorithms for pulse wave analysis. None of the other authors has any conflicts of interest, financial or otherwise, to disclose.

AUTHOR CONTRIBUTIONS

P.H.C., B.P., M.B., M.H., V.D., B.H., D.V., D.Ž., and V.M. conceived and designed research; P.H.C., B.P., K.P., M.B., S.Z., D.K., D.Ž., and V.M., performed experiments; P.H.C., B.P., K.P., M.B., S.Z., D.K., D.Ž., and V.M. analyzed data; P.H.C., B.P., K.P., M.B., S.Z., D.K., J.A., D.V., D.Ž., and

Downloaded from journals.physiology.org/journal/ajpheart (193.219.170.065) on March 9, 2022.

Table A4. *Datasets of PPG signals used to assess PPG-derived parameters of vascular age [Modified from (226)]*

Dataset	Reference	Signals	Reference Parameters	No. Subjects	Description
UK Biobank	(224)	PPG	Blood pressure (BP), chronological age	205,337	Single finger PPG waves from middle-aged subjects. The stiffness index, calculated by the PPG device, is also available.
MIMIC	(225)	PPG, BP, electrocardiogram (ECG), others	BP, ankle-brachial index, chronological age	10,000	Recordings from critically ill adults and neonates, lasting from minutes to days. Typically, at finger.
Cuffless BP Estimation	(226, 227)	PPG, ECG	BP	942	Recordings from critically ill patients, each lasting ≥10 min. Extracted from the MIMIC-II Database.
PPG-BP Database	(228)	PPG	BP, chronological age	219	Three finger recordings from adults aged 20–89 with and without cardiovascular disease, three waves per recording.
University of Queensland Vital Signs Dataset	(229)	PPG, ECG, BP	BP	32	Recordings from patients during anesthesia, ranging from minutes to hours in duration.
Pulse Wave Database	(4, 230)	PPG, BP	BP, pulse wave velocity, chronological age, others	4,374(simulated)	Single simulated PPG pulse waves representative of healthy adults aged 25–75.

BP, blood pressure; PPG, photoplethysmogram

V.M. interpreted results of experiments; P.H.C., K.P., M.B. D.Ž., and V.M. prepared figures; P.H.C., B.P., K.P., M.B., S.Z., D.K., J.A., V.D., D.V., D. Ž., and V.M., drafted manuscript; P.H.C., B.P., K.P., M.B., S.Z., D.K., J.A., E.B., C.C.M., D.T.-P., B.H., D.V., D.Ž., and V.M. edited and revised manuscript; P.H.C., B.P., K.P., M.B., S.Z., D.K., J.A., M.H., E.B., C.C.M., D.T.-P., V.D., B.H., D.V., D.Ž., and V.M., approved final version of manuscript.

REFERENCES

1. **Hamczyk MR**, **Nevado RM**, **Barettino A**, **Fuster V**, **Andrés V.** Biological versus chronological aging: JACC focus seminar. *J Am Coll Cardiol* 75: 919–930, 2020. doi:10.1016/j.jacc.2019.11.062.
2. **O'Rourke M**, **Nichols WW**, **Vlachopoulos C.** *McDonald's Blood Flow in Arteries* (6th ed.). London, UK: Hodder Arnold, 2011.
3. **O'Rourke M.** Arterial stiffness, systolic blood pressure, and logical treatment of arterial hypertension. *Hypertension* 15: 339–347, 1990. doi:10.1161/01.HYP.15.4.339.
4. **Charlton PH**, **Mariscal Harana J**, **Vennin S**, **Li Y**, **Chowienczyk P**, **Alastruey J.** Modeling arterial pulse waves in healthy aging: a database for in silico evaluation of hemodynamics and pulse wave indexes. *Am J Physiol Heart Circ Physiol* 317: H1062–H1085, 2019. doi:10.1152/ajpheart.00218.2019.
5. **Vlachopoulos C**, **Aznaouridis K**, **Stefanadis C.** Prediction of cardiovascular events and all-cause mortality with arterial stiffness: a systematic review and meta-analysis. *J Am Coll Cardiol* 55: 1318–1327, 2010. doi:10.1016/j.jacc.2009.10.061.
6. **Bruno RM**, **Nilsson PM**, **Engström G**, **Wadström BN**, **Empana J-P**, **Boutouyrie P**, **Laurent S.** Early and supernormal vascular aging: clinical characteristics and association with incident cardiovascular events. *Hypertension* 76: 1616–1624, 2020. doi:10.1161/HYPERTENSIONAHA.120.14971.
7. **Miyasaka K**, **Shelley K**, **Takahashi S**, **Kubota H**, **Ito K**, **Yoshiya I**, **Yamanishi A**, **Cooper JB**, **Steward DJ**, **Nishida H**, **Kiani J**, **Ogino H**, **Sata Y**, **Kopotic Rj Jenkin K**, **Hannenberg A. Gawande A.** Tribute to Dr. Takuo Aoyagi, inventor of pulse oximetry. *J Anesth* 35: 671–709, 2021. doi:10.1007/s00540-021-02967-z.[34338865]
8. **Sahli D**, **Eliasson B**, **Svensson M**, **Blohmé G**, **Eliasson M**, **Samuelsson P**, **Öjbrandt K**, **Eriksson JW.** Assessment of toe blood pressure is an effective screening method to identify diabetes patients with lower extremity arterial disease. *Angiology* 55: 641–651, 2004. doi:10.1177/000331970405501605.
9. **Zhang Y**, **Weaver RG**, **Armstrong B**, **Burkart S**, **Zhang S**, **Beets MW.** Validity of Wrist-Worn photoplethysmography devices to measure heart rate: a systematic review and meta-analysis. *J Sports Sci* 38: 2021–2034, 2020. doi:10.1080/02640414.2020.1767348.
10. **The Reference Values for Arterial Stiffness' Collaboration**. Determinants of pulse wave velocity in healthy people and in the presence of cardiovascular risk factors: Establishing normal and reference values. *Eur Heart J* 31: 2338–2350, 2010. doi:10.1093/eurheartj/ehq165.
11. **Allen J**, **Murray A.** Age-related changes in the characteristics of the photoplethysmographic pulse shape at various body sites. *Physiol Meas* 24: 297–307, 2003. doi:10.1088/0967-3334/24/2/306.
12. **Allen J**, **Murray A.** Age-related changes in peripheral pulse timing characteristics at the ears, fingers and toes. *J Hum Hypertens* 16: 711–717, 2002. doi:10.1038/sj.jhh.1001478.
13. **McVeigh GE**, **Bratteli CW**, **Morgan DJ**, **Alinder CM**, **Glasser SP**, **Finkelstein SM**, **Cohn JN.** Age-related abnormalities in arterial compliance identified by pressure pulse contour analysis: aging and arterial compliance. *Hypertension* 33: 1392–1398, 1999. doi:10.1161/01.HYP.33.6.1392.
14. **Hashimoto J**, **Watabe D**, **Kimura A**, **Takahashi H**, **Ohkubo T**, **Totsune K**, **Imai Y.** Determinants of the second derivative of the finger photoplethysmogram and brachial-ankle pulse-wave velocity: the Ohasama study. *Am J Hypertens* 18: 477–485, 2005. doi:10.1016/j.amjhyper.2004.11.009.
15. **Grant MJ**, **Booth A.** A typology of reviews: an analysis of 14 review types and associated methodologies. *Health Info Libr J* 26: 91–108, 2009. doi:10.1111/j.1471-1842.2009.00848.x.
16. **Ouzzani M**, **Hammady H**, **Fedorowicz Z**, **Elmagarmid A.** Rayyan—a web and mobile app for systematic reviews. *Syst Rev* 5: 210, 2016. doi:10.1186/s13643-016-0384-4.
17. **Radha M**, **de Groot K**, **Rajani N**, **Wong CCP**, **Kobold N**, **Vos V**, **Fonseca P**, **Mastellos N**, **Wark PA**, **Velthoven N**, **Haakma R**, **Aarts RM.** Estimating blood pressure trends and the nocturnal dip from photoplethysmography. *Physiol Meas* 40: 025006, 2019. doi:10.1088/1361-6579/ab030e.
18. **Xing X**, **Ma Z**, **Zhang M**, **Gao X**, **Li Y**, **Song M**, **Dong W-FF.** Robust blood pressure estimation from finger photoplethysmography using age-dependent linear models. *Physiol Meas* 41: 025007, 2020. doi:10.1088/1361-6579/ab755d.
19. **Wang Y**, **Chen C**, **Sue C**, **Lu W**, **Chiou Y.** Estimation of blood pressure in the radial artery using strain-based pulse wave and photoplethysmography sensors. *Micromachines* 9: 556, 2018. doi:10.3390/mi9110556.
20. **Cho S I**, **Negishi T**, **Tsuchiya M**, **Yasuda M**, **Yokoyama M.** Estimation system of blood pressure variation with photoplethysmography signals using multiple regression analysis and neural

Downloaded from journals.physiology.org/journal/ajpheart (193.219.170.065) on March 9, 2022.

network. *Int J Fuzzy Log Intell Syst* 18: 229–236, 2018. doi:10.5391/IJFIS.2018.18.4.229.

21. **Liang Y**, **Chen Z**, **Ward R**, **Elgendi M.** Hypertension assessment using photoplethysmography: a risk stratification approach. *J Clin Med* 8: 12, 2018. doi:10.3390/jcm8010012.
22. **Liang Y**, **Chen Z**, **Ward R**, **Elgendi M.** Hypertension assessment via ECG and PPG signals: an evaluation using MIMIC database. *Diagnostics* 8: 65, 2018. doi:10.3390/diagnostics8030065.
23. **Bentham M**, **Stansby G**, **Allen J.** Innovative multi-site photoplethysmography analysis for quantifying pulse amplitude and timing variability characteristics in peripheral arterial disease. *Diseases* 6: 81, 2018. doi:10.3390/diseases6030081.
24. **Sharkey EJ**, **Di Maria C**, **Klinge A**, **Murray A**, **Zheng D**, **O'Sullivan J**, **Allen J.** Innovative multi-site photoplethysmography measurement and analysis demonstrating increased arterial stiffness in paediatric heart transplant recipients. *Physiol Meas* 39: 074007, 2018. doi:10.1088/1361-6579/aac76a.
25. **Wei H-C**, **Xiao M-X**, **Chen H-Y**, **Li Y-Q**, **Wu H-T**, **Sun C-K.** Instantaneous frequency from Hilbert-Huang transformation of digital volume pulse as indicator of diabetes and arterial stiffness in upper-middle-aged subjects. *Sci Rep* 8: 15771, 2018. doi:10.1038/s41598-018-34091-6.
26. **Lin WH**, **Wang H**, **Samuel OW**, **Liu G**, **Huang Z**, **Li G.** New photoplethysmogram indicators for improving cuffless and continuous blood pressure estimation accuracy. *Physiol Meas* 39: 025005, 2018. doi:10.1088/1361-6579/aaa454.
27. **Peltokangas M**, **Telembeci AA**, **Verho J**, **Mattila VM**, **Romsi P**, **Vehkaoja A**, **Lekkala J**, **Oksala N.** Parameters extracted from arterial pulse waves as markers of atherosclerotic changes: performance and repeatability. *IEEE J Biomed Health Inform* 22: 750–757, 2018. doi:10.1109/JBHI.2017.2679904.
28. **Liang Y**, **Chen Z**, **Ward R**, **Elgendi M.** Photoplethysmography and deep learning: enhancing hypertension risk stratification. *Biosensors* 8: 101, 2018. doi:10.3390/bios8040101.
29. **Nitzan M**, **Babchenko A**, **Khanokh B.** Very low frequency variability in arterial blood pressure and blood volume pulse. *Med Biol Eng Comput* 37: 54–58, 1999. doi:10.1007/BF02513266.
30. **Yang C**, **Tavassolian N.** Pulse transit time measurement using seismocardiogram, photoplethysmogram, and acoustic recordings: evaluation and comparison. *IEEE J Biomed Health Inform* 22: 733–740, 2018. doi:10.1109/JBHI.2017.2696703.
31. **Feng J**, **Huang Z**, **Zhou C**, **Ye X.** Study of continuous blood pressure estimation based on pulse transit time, heart rate and photoplethysmography-derived hemodynamic covariates. *Australas Phys Eng Sci Med* 41: 403–413, 2018. doi:10.1007/s13246-018-0637-8.
32. **Lan K. C**, **Raknim P**, **Kao WF**, **Huang JH.** Toward hypertension prediction based on PPG-derived HRV signals: a feasibility study. *J Med Syst* 42: 103, 2018. doi:10.1007/s10916-018-0942-5.
33. **Lazazzera R**, **Belhaj Y**, **Carrault G.** A new wearable device for blood pressure estimation using photoplethysmogram. *Sensors* 19: 2557–2518, 2019. doi:10.3390/s19112557.
34. **Sharifi I**, **Goudarzi S**, **Khodabakhshi MB.** A novel dynamical approach in continuous cuffless blood pressure estimation based on ECG and PPG signals. *Artif Intell Med* 97: 143–151, 2019. doi:10.1016/j.artmed.2018.12.005.
35. **Xing X**, **Ma Z**, **Zhang M**, **Zhou Y**, **Dong W**, **Song M.** An unobtrusive and calibration-free blood pressure estimation method using photoplethysmography and biometrics. *Sci Rep* 9: 8611, 2019. doi:10.1038/s41598-019-45175-2.
36. **von Wowern E**, **Källén K**, **Olofsson P.** Arterial stiffness in normal pregnancy as assessed by digital pulse wave analysis by photoplethysmography—a longitudinal study. *Pregnancy Hypertens* 15: 51–56, 2019. doi:10.1016/j.preghy.2018.11.002.
37. **Murakami T**, **Asai K**, **Kadono Y**, **Nishida T**, **Nakamura H**, **Kishima H.** Assessment of arterial stiffness index calculated from accelerated photoplethysmography. *Artery Res* 25: 37–40, 2019. doi:10.2991/artres.k.191120.001.
38. **Wu JX**, **Lin CH**, **Kan CD**, **Chen WL.** Bilateral photoplethysmography for peripheral arterial disease screening in haemodialysis patients using astable multivibrator and machine learning classifier. *IET Sci Meas Technol* 13: 1277–1286, 2019. doi:10.1049/iet-smt.2018.5330.
39. **Mousavi SS**, **Firouzmand M**, **Charmi M**, **Hemmati M**, **Moghadam M**, **Ghorbani Y.** Blood pressure estimation from appropriate and inappropriate PPG signals using A whole-based method. *Biomed Signal Process Control* 47: 196–206, 2019. doi:10.1016/j.bspc.2018.08.022.
40. **Khalid SG**, **Liu H**, **Zia T**, **Zhang J**, **Chen F**, **Zheng D.** Cuffless blood pressure estimation using single channel photoplethysmography: a two-step method. *IEEE Access* 8: 58146–58154, 2020. doi:10.1109/ACCESS.2020.2981903.
41. **Slapničar G**, **Mlakar N**, **Luštrek M.** Blood pressure estimation from photoplethysmogram using a spectro-temporal deep neural network. *Sensors* 19: 3420, 2019. doi:10.3390/s19153420.
42. **Pour Ebrahim M**, **Heydari F**, **Wu T**, **Walker K**, **Joe K**, **Redoute JM**, **Yuce MR.** Blood pressure estimation using on-body continuous wave radar and photoplethysmogram in various posture and exercise conditions. *Sci Rep* 9: 16346, 2019. doi:10.1038/s41598-019-52710-8.
43. **Kock KDS**, **Silva JD**, **Marques JLB.** Comparison of the ankle-brachial index with parameters of stiffness and peripheral arterial resistance assessed by photoplethysmography in elderly patients. *J Vasc Bras* 18: e20180084, 2019. doi:10.1590/1677-5449.180084.
44. **Fischer C**, **Penzel T.** Continuous non-invasive determination of nocturnal blood pressure variation using photoplethysmographic pulse wave signals: comparison of pulse propagation time, pulse transit time and RR-interval. *Physiol Meas* 40: 014001, 2019. doi:10.1088/1361-6579/aaf298.
45. **Tanveer MS**, **Hasan MK.** Cuffless blood pressure estimation from electrocardiogram and photoplethysmogram using waveform based ANN-LSTM network. *Biomed Signal Process Control* 51: 382–392, 2019. doi:10.1016/j.bspc.2019.02.028.
46. **Yan WR**, **Peng RC**, **Zhang YT**, **Ho D.** Cuffless continuous blood pressure estimation from pulse morphology of photoplethysmograms. *IEEE Access* 7: 141970–141977, 2019. doi:10.1109/ACCESS.2019.2942936.
47. **Chiarelli AM**, **Bianco F**, **Perpetuini D**, **Bucciarelli V**, **Filippini C**, **Cardone D**, **Zappasodi F**, **Gallina S**, **Merla A.** Data-driven assessment of cardiovascular ageing through multisite photoplethysmography and electrocardiography. *Med Eng Phys* 73: 39–50, 2019. doi:10.1016/j.medengphy.2019.07.009.
48. **Peltokangas M**, **Suominen V**, **Vakhitov D**, **Korhonen J**, **Verho J**, **Mattila VM**, **Romsi P**, **Lekkala J**, **Vehkaoja A**, **Oksala N.** Effects of percutaneous transluminal angioplasty of superficial femoral artery on photoplethysmographic pulse transit times. *IEEE J Biomed Health Inform* 23: 1058–1065, 2019. doi:10.1109/JBHI.2018.2851388.
49. **Zekavat SM**, **Aragam K**, **Emdin C**, **Khera AV**, **Klarin D**, **Zhao H**, **Natarajan P.** Genetic association of finger photoplethysmography-derived arterial stiffness index with blood pressure and coronary artery disease. *Arterioscler Thromb Vasc Biol* 39: 1253–1261, 2019. doi:10.1161/ATVBAHA.119.312626.
50. **Hassani A**, **Foruzan AH.** Improved PPG-based estimation of the blood pressure using latent space features. *Signal Image Video Process* 13: 1141–1147, 2019. doi:10.1007/s11760-019-01460-1.
51. **Bortolotto LA**, **Blacher J**, **Kondo T**, **Takazawa K**, **Safar ME.** Assessment of vascular aging and atherosclerosis in hypertensive subjects: second derivative of photoplethysmogram versus pulse wave velocity. *Am J Hypertens* 13: 165–171, 2000. doi:10.1016/S0895-7061(99)00192-2.
52. **Perpetuini D**, **Chiarelli AM**, **Maddiona L**, **Rinella S**, **Bianco F**, **Bucciarelli V**, **Gallina S**, **Perciavalle V**, **Vinciguerra V**, **Merla A**, **Fallica G.** Multi-site photoplethysmographic and electrocardiographic system for arterial stiffness and cardiovascular status assessment. *Sensors* 19: 5570, 2019. doi:10.3390/s19245570.
53. **Liu J**, **Yan BP**, **Zhang Y**, **Ding X**, **Su P**, **Zhao N.** Multi-wavelength photoplethysmography enabling continuous blood pressure measurement with compact wearable electronics. *IEEE Trans Biomed Eng* 66: 1514–1525, 2019. doi:10.1109/TBME.2018.2874957.
54. **Wu H**, **Ji Z**, **Li M.** Non-invasive continuous blood-pressure monitoring models based on photoplethysmography and electrocardiography. *Sensors* 19: 5543, 2019. doi:10.3390/s19245543.
55. **Thambiraj G**, **Gandhi U**, **Devanand V**, **Mangalanathan U.** Noninvasive cuffless blood pressure estimation using pulse transit time, Womersley number, and photoplethysmogram intensity ratio. *Physiol Meas* 40: 075001, 2019. doi:10.1088/1361-6579/ab1f17.
56. **Riaz F**, **Azad MA**, **Arshad J**, **Imran M**, **Hassan A**, **Rehman S.** Pervasive blood pressure monitoring using photoplethysmogram

Downloaded from journals.physiology.org/journal/ajpheart (193.219.170.065) on March 9, 2022.

(PPG) sensor. *Futur Gener Comput Syst* 98: 120–130, 2019. doi:10.1016/j.future.2019.02.032.
57. **Tusman G**, **Acosta CM**, **Pulletz S**, **Böhm SH**, **Scandurra A**, **Arca JM**, **Madorno M**, **Sipmann FS.** Photoplethysmographic characterization of vascular tone mediated changes in arterial pressure: an observational study. *J Clin Monit Comput* 33: 815–824, 2019. doi:10.1007/s10877-018-0235-z.
58. **Gircys R**, **Liutkevicius A**, **Kazanavicius E**, **Lesauskaite V**, **Damuleviciene G**, **Janaviciute A.** Photoplethysmography-based continuous systolic blood pressure estimation method for low processing power wearable devices. *Appl Sci* 9: 2236, 2019. doi:10.3390/app9112236.
59. **Fujita D**, **Suzuki A**, **Ryu K.** PPG-based systolic blood pressure estimation method using PLS and level-crossing feature. *Appl Sci* 9: 304, 2019. doi:10.3390/app9020304.
60. **Dal Pont MP**, **Marques JLB.** Reflective photoplethysmography acquisition platform with monitoring modules and noninvasive blood pressure calculation. *IEEE Trans Instrum Meas* 69: 5649–5657, 2020. doi:10.1109/TIM.2019.2963508.
61. **Kei Fong MW**, **Ng EY**, **Er Zi Jian K**, **Hong TJ.** SVR ensemble-based continuous blood pressure prediction using multi-channel photoplethysmogram. *Comput Biol Med* 113: 103392, 2019. doi:10.1016/j.compbiomed.2019.103392.
62. **Allen J**, **Hedley S.** Simple photoplethysmography pulse encoding technique for communicating the detection of peripheral arterial disease—a proof of concept study. *Physiol Meas* 40: 08NT01, 2019. doi:10.1088/1361-6579/ab3545.
63. **Zhang Q**, **Xie Q**, **Duan K**, **Liang B**, **Wang M**, **Wang G.** A digital signal processor (DSP)-based system for embedded continuous-time cuffless blood pressure monitoring using single-channel PPG signal. *Sci China Inf Sci* 63: 1–3, 2020. doi:10.1007/s11432-018-9719-9.
64. **Esmaelpoor J**, **Moradi MH**, **Kadkhodamohammadi A.** A multistage deep neural network model for blood pressure estimation using photoplethysmogram signals. *Comput Biol Med* 120: 103719, 2020. doi:10.1016/j.compbiomed.2020.103719.
65. **Carek AM**, **Jung H**, **Inan OT.** A reflective photoplethysmogram array and channel selection algorithm for weighing scale based blood pressure measurement. *IEEE Sens J* 20: 3849–3858, 2020. doi:10.1109/JSEN.2019.2960063.
66. **Hasanzadeh N**, **Ahmadi MM**, **Mohammadzade H.** Blood pressure estimation using photoplethysmogram signal and its morphological features. *IEEE Sens J* 20: 4300–4310, 2020. doi:10.1109/JSEN.2019.2961411.
67. **Yang S**, **Zaki WSW**, **Morgan SP**, **Cho SY**, **Correia R**, **Zhang Y.** Blood pressure estimation with complexity features from electrocardiogram and photoplethysmogram signals. *Opt Quantum Electron* 52: 1–16, 2020. doi:10.1007/s11082-020-2260-7.
68. **Marzorati D**, **Bovio D**, **Salito C**, **Mainardi L**, **Cerveri P.** Chest wearable apparatus for cuffless continuous blood pressure measurements based on PPG and PCG signals. *IEEE Access* 8: 55424–55437, 2020. doi:10.1109/ACCESS.2020.2981300.
69. **Chowdhury MH**, **Shuzan MNI**, **Chowdhury MEH**, **Mahbub ZB**, **Monir Uddin M**, **Khandakar A**, **Reaz MBI.** Estimating blood pressure from the photoplethysmogram signal and demographic features using machine learning techniques. *Sensors* 20: 3127, 2020. doi:10.3390/s20113127.
70. **Schlesinger O**, **Vigderhouse N**, **Moshe Y**, **Eytan D.** Estimation and tracking of blood pressure using routinely acquired photoplethysmographic signals and deep neural networks. *Crit Care Explor* 2: e0095, 2020. doi:10.1097/cce.0000000000000095.
71. **Shin YS.** Identification of blood pressure reflecting personalized traits using bilateral photoplethysmography. *Technol Health Care*, 28: 217–227, 2020. doi:10.3233/THC-209022.
72. **Thambiraj G**, **Gandhi U**, **Mangalanathan U**, **Jose VJM**, **Anand M.** Investigation on the effect of Womersley number, ECG and PPG features for cuff less blood pressure estimation using machine learning. *Biomed Signal Process Control* 60: 101942, 2020. doi:10.1016/j.bspc.2020.101942.
73. **Millasseau SC**, **Kelly RP**, **Ritter JM**, **Chowienczyk PJ.** Determination of age-related increases in large artery stiffness by digital pulse contour analysis. *Clin Sci* 103: 371–377, 2002. doi:10.1042/cs1030371.
74. **Tjahjadi R.** Noninvasive blood pressure classification based on photoplethysmography using k-nearest neighbors algorithm: a feasibility study. *Information* 11: 93, 2020. doi:10.3390/info11020093.
75. **Tjahjadi H**, **Ramli K**, **Murfi H.** Noninvasive classification of blood pressure based on photoplethysmography signals using bidirectional long short-term memory and time-frequency analysis. *IEEE Access* 8: 20735–20748, 2020. doi:10.1109/ACCESS.2020.2968967.
76. **Perpetuini D**, **Chiarelli AM**, **Cardone D**, **Rinella S**, **Massimino S**, **Bianco F**, **Bucciarelli V**, **Vinciguerra V**, **Fallica G**, **Perciavalle V**, **Gallina S**, **Merla A.** Photoplethysmographic prediction of the ankle-brachial pressure index through a machine learning approach. *Appl Sci* 10: 2137, 2020. doi:10.3390/app10062137.
77. **Panwar M**, **Gautam A**, **Biswas D**, **Acharyya A.** PP-Net: a deep learning framework for ppg-based blood pressure and heart rate estimation. *IEEE Sens J* 20: 10000–10011, 2020. doi:10.1109/JSEN.2020.2990864.
78. **Chandrasekhar A**, **Yavarimanesh M**, **Natarajan K**, **Hahn J-O**, **Mukkamala R.** PPG sensor contact pressure should be taken into account for cuff-less blood pressure measurement. *IEEE Trans Biomed Eng* 67: 3134–3140, 2020. doi:10.1109/TBME.2020.2976989.
79. **Joachim J**, **Coutrot M**, **Millasseau S**, **Matéo J**, **Mebazaa A**, **Gayat E**, **Vallée F.** Real-time estimation of mean arterial blood pressure based on photoplethysmography dicrotic notch and perfusion index. A pilot study. *J Clin Monit Comput* 35: 395–404, 2021. doi:10.1007/s10877-020-00486-y.
80. **Shalom E**, **Hirshtal E**, **Slotki I**, **Shavit L**, **Yitzhaky Y**, **Engelberg S**, **Nitzan M.** Systolic blood pressure measurement by detecting the photoplethysmographic pulses and electronic Korotkoff-sounds during cuff deflation. *Physiol Meas* 41: 034001, 2020. doi:10.1088/1361-6579/ab7b41.
81. **Kiselev AR**, **Karavaev AS.** The intensity of oscillations of the photoplethysmographic waveform variability at frequencies 0.04–0.4 Hz is effective marker of hypertension and coronary artery disease in males. *Blood Press* 29: 55–62, 2020. doi:10.1080/08037051.2019.1645586.
82. **Kuznetsova T**, **Van Vlierberghe E**, **Knez J**, **Szczesny G**, **Thijs L**, **Jozeau D**, **Balestra C**, **D'Hooge J**, **Staessen JA.** Association of digital vascular function with cardiovascular risk factors: a population study. *BMJ Open* 4: e004399, 2014. doi:10.1136/bmjopen-2013-004399.
83. **Allen J**, **O'Sullivan J**, **Stansby G**, **Murray A.** Age-related changes in pulse risetime measured by multi-site photoplethysmography. *Physiol Meas* 41: 074001, 2020. doi:10.1088/1361-6579/ab9b67.
84. **Hashimoto J**, **Chonan K**, **Aoki Y**, **Nishimura T**, **Ohkubo T**, **Hozawa A**, **Suzuki M**, **Matsubara M**, **Michimata M**, **Araki T**, **Imai Y.** Pulse wave velocity and the second derivative of the finger photoplethysmogram in treated hypertensive patients: their relationship and associating factors. *J Hypertens* 20: 2415–2422, 2002. doi:10.1097/00004872-200212000-00021.
85. **Kulin D**, **Antali F**, **Kulin S**, **Wafa D**, **Lucz KI**, **Veres DS**, **Miklós Z.** Preclinical, multi-aspect assessment of the reliability of a photoplethysmography-based telemonitoring system to track cardiovascular status. *Appl Sci* 10: 7977–7917, 2020. doi:10.3390/app10227977.
86. **Alivon M**, **Phuong TVD**, **Vignon V**, **Bozec E**, **Khettab H**, **Hanon O**, **Briet M**, **Halimi JM**, **Hallab M**, **Plichart M**, **Mohammedi K**, **Marre M**, **Boutouyrie P**, **Laurent S.** A novel device for measuring arterial stiffness using finger-toe pulse wave velocity: validation study of the pOpmètre®. *Arch Cardiovasc Dis* 108: 227–234, 2015. doi:10.1016/j.acvd.2014.12.003.
87. **Nitzan M**, **Khanokh B**, **Slovik Y.** The difference in pulse transit time to the toe and finger measured by photoplethysmography. *Physiol Meas* 23: 85–93, 2002. doi:10.1088/0967-3334/23/1/308.
88. **Takazawa K**, **Tanaka N**, **Fujita M**, **Matsuoka O**, **Saiki T**, **Aikawa M**, **Tamura S**, **Ibukiyama C.** Assessment of vasoactive agents and vascular aging by the second derivative of photoplethysmogram waveform. *Hypertension* 32: 365–370, 1998. doi:10.1161/01.HYP.32.2.365.
89. **Loukogeorgakis S**, **Dawson R**, **Phillips N**, **Martyn CN**, **Greenwald SE.** Validation of a device to measure arterial pulse wave velocity by a photoplethysmographic method. *Physiol Meas* 23: 581–596, 2002. doi:10.1088/0967-3334/23/3/309.
90. **Pilt K**, **Ferenets R**, **Meigas K**, **Lindberg L-G**, **Temitski K**, **Viigimaa M.** New photoplethysmographic signal analysis algorithm for arterial stiffness estimation. *Sci World J* 2013: 1–9, 2013. doi:10.1155/2013/169035.
91. **Millasseau SC**, **Kelly RP**, **Ritter JM**, **Chowienczyk PJ.** The vascular impact of aging and vasoactive drugs: comparison of two digital

Downloaded from journals.physiology.org/journal/ajpheart (193.219.170.065) on March 9, 2022.

volume pulse measurements. *Am J Hypertens* 16: 467–472, 2003. doi:10.1016/S0895-7061(03)00569-7.
92. **Foo JYA**, **Wilson SJ**, **Williams GR**, **Harris M**, **Cooper DM.** Motion artefact reduction of the photoplethysmographic signal in pulse transit time measurement. *Australas Phys Eng Sci Med* 27: 165–173, 2004. doi:10.1007/BF03178645.
93. **Ubbink DT.** Toe blood pressure measurements in patients suspected of leg ischaemia: a new laser Doppler device compared with photoplethysmography. *Eur J Vasc Endovasc Surg* 27: 629–634, 2004. doi:10.1016/j.ejvs.2004.01.031.
94. **Tsai WC**, **Chen JY**, **Wang MC**, **Wu HT**, **Chi CK**, **Chen YK**, **Chen JH**, **Lin LJ.** Association of risk factors with increased pulse wave velocity detected by a novel method using dual-channel photoplethysmography. *Am J Hypertens* 18: 1118–1122, 2005. doi:10.1016/j.amjhyper.2005.03.739.
95. **Jönsson B**, **Laurent C**, **Eneling M**, **Skau T**, **Lindberg L-G.** Automatic ankle pressure measurements using PPG in ankle-brachial pressure index determination. *Eur J Vasc Endovasc Surg* 30: 395–401, 2005. doi:10.1016/j.ejvs.2005.05.012.
96. **Brumfield AM**, **Andrew ME.** Digital pulse contour analysis: investigating age-dependent indices of arterial compliance. *Physiol Meas* 26: 599–608, 2005. doi:10.1088/0967-3334/26/5/003.
97. **Laurent C**, **Jönsson B**, **Vegfors M**, **Lindberg LG.** Non-invasive measurement of systolic blood pressure on the arm utilising photoplethysmography: development of the methodology. *Med Biol Eng Comput* 43: 131–135, 2005. doi:10.1007/BF02345134.
98. **Allen J**, **Oates CP**, **Lees TA**, **Murray A.** Photoplethysmography detection of lower limb peripheral arterial occlusive disease: a comparison of pulse timing, amplitude and shape characteristics. *Physiol Meas* 26: 811–821, 2005. doi:10.1088/0967-3334/26/5/018.
99. **Chen JY**, **Tsai WC**, **Lin CC**, **Huang YY**, **Hsu CH**, **Liu PY**, **Chen JH.** Stiffness index derived from digital volume pulse as a marker of target organ damage in untreated hypertension. *Blood Press* 14: 233–237, 2005. doi:10.1080/08037050510034301.
100. **Sollinger D**, **Mohaupt MG**, **Wilhelm A**, **Uehlinger D**, **Frey FJ**, **Eisenberger U.** Arterial stiffness assessed by digital volume pulse correlates with comorbidity in patients with ESRD. *Am J Kidney Dis* 48: 456–463, 2006. doi:10.1053/j.ajkd.2006.05.014.
101. **Dillon JB**, **Hertzman AB.** The form of the volume pulse in the finger pad in health, arteriosclerosis, and hypertension. *Am Heart J* 21: 172–190, 1941. doi:10.1016/S0002-8703(41)90966-3.
102. **Foo JYA**, **Lim CS.** Dual-channel photoplethysmography to monitor local changes in vascular stiffness. *J Clin Monit Comput* 20: 221–227, 2006. doi:10.1007/s10877-006-9024-1.
103. **Zahedi E**, **Chellappan K**, **Ali MAM**, **Singh H.** Analysis of the effect of ageing on rising edge characteristics of the photoplethysmogram using a modified windkessel model. *Cardiovasc Eng* 7: 172–181, 2007. doi:10.1007/s10558-007-9037-5.
104. **Otsuka T**, **Kawada T**, **Katsumata M**, **Ibuki C**, **Kusama Y.** Independent determinants of second derivative of the finger photoplethysmogram among various cardiovascular risk factors in middle-aged men. *Hypertens Res* 30: 1211–1218, 2007. doi:10.1291/hypres.30.1211.
105. **Alty SR**, **Angarita-Jaimes N**, **Millasseau SC**, **Chowienczyk PJ.** Predicting arterial stiffness from the digital volume pulse waveform. *IEEE Trans Biomed Eng* 54: 2268–2275, 2007. doi:10.1109/TBME.2007.897805.
106. **Allen J**, **Overbeck K**, **Nath AF**, **Murray A**, **Stansby G.** A prospective comparison of bilateral photoplethysmography versus the ankle-brachial pressure index for detecting and quantifying lower limb peripheral arterial disease. *J Vasc Surg* 47: 794–802, 2008. doi:10.1016/j.jvs.2007.11.057.
107. **Brillante DG**, **O'Sullivan AJ**, **Howes LG.** Arterial stiffness indices in healthy volunteers using non-invasive digital photoplethysmography. *Blood Press* 17: 116–123, 2008. doi:10.1080/08037050802059225.
108. **Gunarathne A**, **Patel JV**, **Hughes E. A**, **Lip GYH.** Measurement of stiffness index by digital volume pulse analysis technique: clinical utility in cardiovascular disease risk stratification. *Am J Hypertens* 21: 866–872, 2008. doi:10.1038/ajh.2008.207.
109. **Jayasree V**, **Sandhya T**, **Radhakrishnan P.** Non-invasive studies on age related parameters using a blood volume pulse sensor. *Meas Sci Rev* 8: 82–86, 2008. doi:10.2478/v10048-008-0020-0.
110. **Simonetti GD**, **Eisenberger U**, **Bergmann IP**, **Frey FJ**, **Mohaupt MG.** Pulse contour analysis: a valid assessment of central arterial stiffness in children? *Pediatr Nephrol* 23: 439–444, 2008. doi:10.1007/s00467-007-0693-x.
111. **Nitzan M**, **Patron A**, **Glik Z**, **Weiss AT.** Automatic noninvasive measurement of systolic blood pressure using photoplethysmography. *Biomed Eng Online* 8: 28, 2009. doi:10.1186/1475-925X-8-28.
112. **Rajala S**, **Lindholm H**, **Taipalus T.** Comparison of photoplethysmogram measured from wrist and finger and the effect of measurement location on pulse arrival time. *Physiol Meas* 39: 075010, 2018. doi:10.1088/1361-6579/aac7ac.
113. **Jaffer U**, **Aslam M**, **Standfield N.** Comparison of Doppler ultrasound, photoplethysmographic, and pulse-oximetric calculated pressure indices to detect peripheral arterial occlusive disease. *Vasc Dis Manag* 6: 100–105, 2009.
114. **Yoon Y**, **Cho JH**, **Yoon G.** Non-constrained blood pressure monitoring using ECG and PPG for personal healthcare. *J Med Syst* 33: 261–266, 2009. doi:10.1007/s10916-008-9186-0.
115. **Padilla JM**, **Berjano EJ**, **Sáiz J**, **Rodriguez R**, **Fácila L.** Pulse wave velocity and digital volume pulse as indirect estimators of blood pressure: pilot study on healthy volunteers. *Cardiovasc Eng* 9: 104–112, 2009. doi:10.1007/s10558-009-9080-5.
116. **Tanaka G**, **Yamakoshi K**, **Sawada Y**, **Matsumura K**, **Maeda K**, **Kato Y**, **Horiguchi M**, **Ohguro H.** A novel photoplethysmography technique to derive normalized arterial stiffness as a blood pressure independent measure in the finger vascular bed. *Physiol Meas* 32: 1869–1883, 2011. doi:10.1088/0967-3334/32/11/003.
117. **Lin CH.** Assessment of bilateral photoplethysmography for lower limb peripheral vascular occlusive disease using color relation analysis classifier. *Comput Methods Programs Biomed* 103: 121–131, 2011. doi:10.1016/j.cmpb.2010.06.014.
118. **Kuznetsova T**, **Szczesny G**, **Thijs L**, **Jozeau D**, **D'hooge J**, **Staessen JA.** Assessment of peripheral vascular function with photoplethysmographic pulse amplitude. *ARTRES* 5: 58–64, 2011. doi:10.1016/j.artres.2011.03.001.
119. **Wang M**, **Wu A**, **Cheng M**, **Chen J**, **Ho C**, **Tsai W.** Association of arterial stiffness indexes, determined from digital volume pulse measurement and cardiovascular risk factors in chronic kidney disease. *Am J Hypertens* 24: 544–549, 2011. doi:10.1038/ajh.2010.266.
120. **Solà J**, **Chételat O**, **Sartori C**, **Allemann Y**, **Rimoldi SF.** Chest pulse-wave velocity: a novel approach to assess arterial stiffness. *IEEE Trans Biomed Eng* 58: 215–223, 2011. doi:10.1109/TBME.2010.2071385.
121. **Liu AB**, **Hsu PC**, **Chen ZL**, **Wu HT.** Measuring pulse wave velocity using ECG and photoplethysmography. *J Med Syst* 35: 771–777, 2011. doi:10.1007/s10916-010-9469-0.
122. **Clarenbach CF**, **Stoewhas A-C**, **Van Gestel AJ**, **Latshang TD**, **Lo Cascio CM**, **Bloch KE**, **Kohler M.** Comparison of photoplethysmographic and arterial tonometry-derived indices of arterial stiffness. *Hypertens Res* 35: 228–233, 2012. doi:10.1038/hr.2011.168.
123. **Sherebrin MH**, **Sherebrin RZ.** Frequency analysis of the peripheral pulse wave detected in the finger with a photoplethysmograph. *IEEE Trans Biomed Eng* 37: 313–317, 1990. doi:10.1109/10.52332.
124. **Scanlon C**, **Park K**, **Mapletoft D**, **Begg L**, **Burns J.** Interrater and intrarater reliability of photoplethysmography for measuring toe blood pressure and toe-brachial index in people with diabetes mellitus. *J Foot Ankle Res* 5: 13, 2012. doi:10.1186/1757-1146-5-13.
125. **Yousef Q**, **Reaz MBI**, **Ali MAM.** The analysis of PPG morphology: investigating the effects of aging on arterial compliance. *Meas Sci Rev* 12: 266–271, 2012. doi:10.2478/v10048-012-0036-3.
126. **Huotari M**, **Vehkaoja A**, **Määttä K**, **Kostamovaara J**, **Röning J.** Arterial pulse waves measured with EMFi and PPG sensors and comparison of the pulse waveform spectral and decomposition analysis in healthy young and elderly subjects. *WIT Trans Biomed Health* 17: 3–11, 2013. doi:10.2495/BIO130011.
127. **Wei CC.** Developing an effective arterial stiffness monitoring system using the spring constant method and photoplethysmography. *IEEE Trans Biomed Eng* 60: 151–154, 2013. doi:10.1109/TBME.2012.2207384.
128. **Uangpairoj P**, **Shibata M.** Evaluation of vascular wall elasticity of human digital arteries using alternating current-signal photoplethysmography. *Vasc Health Risk Manag* 9: 283–295, 2013. doi:10.2147/vhrm.s43784.
129. **Ro DH**, **Moon HJ**, **Kim JH**, **Lee KM**, **Kim SJ**, **Lee DY.** Photoplethysmography and continuous-wave doppler ultrasound as a complementary test to ankle-brachial index in detection of

Downloaded from journals.physiology.org/journal/ajpheart (193.219.170.065) on March 9, 2022.

stenotic peripheral arterial disease. *Angiology* 64: 314–320, 2013. doi:10.1177/0003319712464814.
130. **Sangle SR**, **Tanikawa A**, **Schreiber K**, **Zakalka M**, **D'Cruz DP.** The prevalence of abnormal pulse wave velocity, pulse contour analysis and ankle-brachial index in patients with livedo reticularis: a controlled study. *Rheumatology (Oxford)* 52: 1992–1998, 2013. doi:10.1093/rheumatology/ket227.
131. **Li Y**, **Wang Z**, **Zhang L**, **Yang X**, **Song J.** Characters available in photoplethysmogram for blood pressure estimation: beyond the pulse transit time. *Australas Phys Eng Sci Med* 37: 367–376, 2014. doi:10.1007/s13246-014-0269-6.
132. **Usman S**, **Reaz MBI**, **Ali MAM.** Determining the arterial stiffness through contour analysis of a PPG and its association with HbA1c among diabetic patients in Malaysia. *Acta Sci Technol* 36: 123–128, 2013. doi:10.4025/actascitechnol.v36i1.17096.
133. **Pilt K**, **Meigas K**, **Kööts K**, **Viigimaa M.** Photoplethysmographic signal rising front analysis for the discrimination of subjects with increased arterial ageing. *Proc Est Acad Sci* 63: 309–314, 2014. doi:10.3176/proc.2014.3.03.
134. **Ponzetto M**, **Neirotti M**, **Romin R**, **Marabotto M**, **Massaia M**, **Scarafiotti C**, **Molaschi M.** Hemorheolocical and photoplethysmographical modifications with aging. *Arch Gerontol Geriatr* 22: 207–211, 1996. doi:10.1016/0167-4943(96)86937-8.
135. **Pilt K**, **Meigas K**, **Ferenets R**, **Temitski K**, **Viigimaa M.** Photoplethysmographic signal waveform index for detection of increased arterial stiffness. *Physiol Meas* 35: 2027–2036, 2014. doi:10.1088/0967-3334/35/10/2027.
136. **He X**, **Goubran RA**, **Liu XP.** Secondary peak detection of PPG signal for continuous cuffless arterial blood pressure measurement. *IEEE Trans Instrum Meas* 63: 1431–1439, 2014. doi:10.1109/TIM.2014.2299524.
137. **Hong KS**, **Park KT**, **Ahn JM.** Aging index using photoplethysmography for a healthcare device: comparison with brachial-ankle pulse wave velocity. *Healthc Inform Res* 21: 30–34, 2015. doi:10.4258/hir.2015.21.1.30.
138. **Xu L**, **Gao K.** Continuous cuffless arterial blood pressure measurement based on PPG quality assessment. *Int J Comput Biol Drug Des* 8: 150–158, 2015. doi:10.1504/IJCBDD.2015.071170.
139. **Von Wowern E**, **Östling G**, **Nilsson PM**, **Olofsson P.** Digital photoplethysmography for assessment of arterial stiffness: repeatability and comparison with applanation tonometry. *PLoS One* 10: e0135659–19, 2015. doi:10.1371/journal.pone.0135659.
140. **Jang DG**, **Park SH**, **Hahn M.** Enhancing the pulse contour analysis-based arterial stiffness estimation using a novel photoplethysmographic parameter. *IEEE J Biomed Health Inform* 19: 256–262, 2015. doi:10.1109/JBHI.2014.2306679.
141. **Zahedi E**, **Sohani V**, **Mohd. Ali MA**, **Chellappan K**, **Beng GK.** Experimental feasibility study of estimation of the normalized central blood pressure waveform from radial photoplethysmogram. *J Healthc Eng* 6: 121–144, 2015. doi:10.1260/2040-2295.6.1.121.
142. **Suzuki A.** Inverse-model-based cuffless blood pressure estimation using a single photoplethysmography sensor. *Proc Inst Mech Eng H* 229: 499–505, 2015. doi:10.1177/0954411915587957.
143. **Matheus A. D M**, **Pires BP**, **Tibiriçá E**, **Silva ATK**, **Gomes MB.** Assessment of arterial stiffness in type 1 diabetes using digital pulse contour analysis: is it a reliable method? *Acta Diabetol* 53: 477–482, 2016. doi:10.1007/s00592-015-0821-1.
144. **Wu JX**, **Li CM**, **Ho YR**, **Wu MJ**, **Huang PT**, **Lin CH.** Bilateral photoplethysmography analysis for peripheral arterial stenosis screening with a fractional-order integrator and info-gap decision-making. *IEEE Sens J* 16: 2691–2700, 2016. doi:10.1109/JSEN.2015.2513899.
145. **López-Beltrán EA**, **Blackshear PL**, **Finkelstein SM**, **Cohn JN.** Non-invasive studies of peripheral vascular compliance using a non-occluding photoplethysmographic method. *Med Biol Eng Comput* 36: 748–753, 1998. doi:10.1007/BF02518879.
146. **Ding X-R**, **Zhang Y-T**, **Liu J**, **Dai W-X**, **Tsang HK.** Continuous cuffless blood pressure estimation using pulse transit time and photoplethysmogram intensity ratio. *IEEE Trans Biomed Eng* 63: 964–972, 2016. doi:10.1109/TBME.2015.2480679.
147. **Vimal Prabhu P**, **Sivaraman J**, **Sathish S**, **Vinurajkumar S**, **Manikandan K.** Detection and evaluation of vascular wall elasticity using photoplethysmography signals in sinus rhythm subjects. *Indian J Sci Technol* 9: 1–5, 2016. doi:10.17485/ijst/2016/v9i2/85811.
148. **Pielmuş AG**, **Pflugradt M**, **Tigges T**, **Klum M**, **Feldheiser A**, **Hunsicker O**, **Orglmeister R.** Novel computation of pulse transit time from multi-channel PPG signals by wavelet transform. *Curr Dir Biomed Eng* 2: 209–213, 2016. doi:10.1515/cdbme-2016-0047.
149. **Li P**, **Liu M**, **Zhang X**, **Hu X**, **Pang B**, **Yao Z**, **Chen H.** Novel wavelet neural network algorithm for continuous and noninvasive dynamic estimation of blood pressure from photoplethysmography. *Sci China Inf Sci* 59: 042405, 2016. doi:10.1007/s11432-015-5400-0.
150. **Xing X**, **Sun M.** Optical blood pressure estimation with photoplethysmography and FFT-based neural networks. *Biomed Opt Express* 7: 3007–3020, 2016. doi:10.1364/BOE.7.003007.
151. **Sun S**, **Bezemer R**, **Long X**, **Muehlsteff J**, **Aarts RM.** Systolic blood pressure estimation using PPG and ECG during physical exercise. *Physiol Meas* 37: 2154–2169, 2016. doi:10.1088/0967-3334/37/12/2154.
152. **Zhang Q**, **Zeng X**, **Hu W**, **Zhou D.** A machine learning-empowered system for long-term motion-tolerant wearable monitoring of blood pressure and heart rate with ear-ECG/PPG. *IEEE Access* 5: 10547–10561, 2017. doi:10.1109/ACCESS.2017.2707472.
153. **Peltokangas M**, **Vehkaoja A**, **Verho J**, **Mattila VM**, **Romsi P**, **Lekkala J**, **Oksala N.** Age dependence of arterial pulse wave parameters extracted from dynamic blood pressure and blood volume pulse waves. *IEEE J Biomed Health Inform* 21: 142–149, 2017. doi:10.1109/JBHI.2015.2503889.
154. **Kern F**, **Bernhard S.** Beat-to-beat blood pressure measurement from instantaneous harmonic phase-shifts in non-invasive photoplethysmographic signals. *Curr Dir Biomed Eng* 3: 755–758, 2017. doi:10.1515/cdbme-2017-0159.
155. **Høyer C**, **Nielsen NS**, **Jordansen MKO**, **Zacho HD.** Comparison of two methods based on photoplethysmography for the diagnosis of peripheral arterial disease. *Scand J Clin Lab Invest* 77: 622–627, 2017. doi:10.1080/00365513.2017.1390784.
156. **Buclin T**, **Buchwalder-Csajka C**, **Brunner HR**, **Biollaz J.** Evaluation of noninvasive blood pressure recording by photoplethysmography in clinical studies using angiotensin challenges. *Br J Clin Pharmacol* 48: 586–593, 1999. doi:10.1046/j.1365-2125.1999.00049.x.
157. **Xu Z**, **Liu J**, **Chen X**, **Wang Y**, **Zhao Z.** Continuous blood pressure estimation based on multiple parameters from eletrocardiogram and photoplethysmogram by back-propagation neural network. *Comput Ind* 89: 50–59, 2017. doi:10.1016/j.compind.2017.04.003.
158. **Choi W**, **Cho JH.** Correlation of peak time shift in blood pressure waveform and ppg based on compliance change analysis in RLC windkessel model. *Curr Opt Photonics* 1: 529–537, 2017. doi:10.3807/COPP.2017.1.5.529.
159. **Wu HT**, **Lee KW**, **Pan WY**, **Liu AB**, **Sun CK.** Difference in bilateral digital volume pulse as a novel non-invasive approach to assessing arteriosclerosis in aged and diabetic subjects: a preliminary study. *Diab Vasc Dis Res* 14: 254–257, 2017. doi:10.1177/1479164116688870.
160. **Rapalis A**, **Janušauskas A**, **Marozas V**, **Lukoševičius A.** Estimation of blood pressure variability during orthostatic test using instantaneous photoplethysmogram frequency and pulse arrival time. *Biomed Signal Process Control* 32: 82–89, 2017. doi:10.1016/j.bspc.2016.10.014.
161. **Obeid H**, **Khettab H**, **Marais L**, **Hallab M**, **Laurent S**, **Boutouyrie P.** Evaluation of arterial stiffness by finger-toe pulse wave velocity: optimization of signal processing and clinical validation. *J Hypertens* 35: 1618–1625, 2017. doi:10.1097/HJH.0000000000001371.
162. **Shin H**, **Min SD.** Feasibility study for the non-invasive blood pressure estimation based on ppg morphology: normotensive subject study. *Biomed Eng Online* 16: 10, 2017. doi:10.1186/s12938-016-0302-y.
163. **Zhang Q**, **Zhou D**, **Zeng X.** Highly wearable cuff-less blood pressure and heart rate monitoring with single-arm electrocardiogram and photoplethysmogram signals. *Biomed Eng Online* 16: 23, 2017. doi:10.1186/s12938-017-0317-z.
164. **Zhang X**, **Ding Q.** Respiratory rate estimation from the photoplethysmogram via joint sparse signal reconstruction and spectra fusion. *Biomed Signal Process Control* 35: 1–7, 2017. doi:10.1016/j.bspc.2017.02.003.
165. **Ahn JM.** New aging index using signal features of both photoplethysmograms and acceleration plethysmograms. *Healthc Inform Res* 23: 53–59, 2017. doi:10.4258/hir.2017.23.1.53.

Downloaded from journals.physiology.org/journal/ajpheart (193.219.170.065) on March 9, 2022.

166. **Bereksi-Reguig MA**, **Bereksi-Reguig F.** Photoplethysmogram signal processing and analysis in evaluating arterial stiffness. *Int J Biomed Eng Technol* 23: 363–378, 2017. doi:10.1504/ijbet.2017.10003507.
167. **Chowienczyk PJ**, **Kelly RP**, **MacCallum H**, **Millasseau SC**, **Andersson TLG**, **Gosling RG**, **Ritter JM**, **änggård EE.** Photoplethysmographic assessment of pulse wave reflection: blunted response to endothelium-dependent beta2-adrenergic vasodilation in type II diabetes mellitus. *J Am Coll Cardiol* 34: 2007–2014, 1999. doi:10.1016/S0735-1097(99)00441-6.
168. **Trumpp A**, **Rasche S**, **Wedekind D**, **Rudolf M**, **Malberg H**, **Matschke K**, **Zaunseder S.** Relation between pulse pressure and the pulsation strength in camera-based photoplethysmograms. *Curr Dir Biomed Eng* 3: 489–492, 2017. doi:10.1515/cdbme-2017-0184.
169. **Inoue N**, **Kawakami H**, **Yamamoto H**, **Ito C**, **Fujiwara S**, **Sasaki H**, **Kihara Y.** Second derivative of the finger photoplethysmogram and cardiovascular mortality in middle-aged and elderly Japanese women. *Hypertens Res* 40: 207–211, 2017. doi:10.1038/hr.2016.123.
170. **Nabeel PM**, **Jayaraj J**, **Mohanasankar S.** Single-source PPG-based local pulse wave velocity measurement: a potential cuffless blood pressure estimation technique. *Physiol Meas* 38: 2122–2140, 2017. doi:10.1088/1361-6579/aa9550.
171. **Kim WJ**, **Kim JW**, **Moon YJ**, **Kim SH**, **Hwang GS**, **Shin WJ.** The photoplethysmographic amplitude to pulse pressure ratio can track sudden changes in vascular compliance and resistance during liver graft reperfusion. *Medicine (United States)* 96, 2017. doi:10.1097/MD.0000000000007045.
172. **Sameen AZ**, **Jaafar R**, **Zahedi E**, **Beng GK.** A novel waveform mirroring technique for systolic blood pressure estimation. *J Eng Sci Technol* 13: 3252–3262, 2018.
173. **Nabeel PM**, **Karthik S**, **Joseph J**, **Sivaprakasam M.** Arterial blood pressure estimation from local pulse wave velocity using dual-element photoplethysmograph probe. *IEEE Trans Instrum Meas* 67: 1399–1408, 2018. doi:10.1109/TIM.2018.2800539.
174. **Soltan Zadi A**, **Alex R**, **Zhang R**, **Watenpaugh DE**, **Behbehani K.** Arterial blood pressure feature estimation using photoplethysmography. *Comput Biol Med* 102: 104–111, 2018. doi:10.1016/j.compbiomed.2018.09.013.
175. **Khalid SG**, **Zhang J**, **Chen F**, **Zheng D.** Blood pressure estimation using photoplethysmography only: comparison between different machine learning approaches. *J Healthc Eng* 2018: 1–13, 2018. doi:10.1155/2018/1548647.
176. **Slapničar G**, **Luštrek M**, **Marinko M.** *Continuous Blood Pressure Estimation from PPG Signal (Online). Informatica* 42: 33–42, 2018. http://www.informatica.si/index.php/informatica/article/view/2229.
177. **Wang Y**, **Liu Z**, **Ma S.** Cuff-less blood pressure measurement from dual-channel photoplethysmographic signals via peripheral pulse transit time with singular spectrum analysis. *Physiol Meas* 39: 025010, 2018. doi:10.1088/1361-6579/aa996d.
178. **Xiao H**, **Butlin M**, **Tan I**, **Avolio A.** Effects of cardiac timing and peripheral resistance on measurement of pulse wave velocity for assessment of arterial stiffness. *Sci Rep* 7: 5990, 2017. doi:10.1038/s41598-017-05807-x.
179. **Lim SS**, **Vos T**, **Flaxman AD**, **Danaei G**, **Shibuya K**, **Adair-Rohani H** et al**.** A comparative risk assessment of burden of disease and injury attributable to 67 risk factors and risk factor clusters in 21 regions, 1990-2010: a systematic analysis for the Global Burden of Disease Study 2010. *Lancet* 380: 2224–2260, 2012. [Erratum in *Lancet* 381: 1276, 2013]. doi:10.1016/S0140-6736(12)61766-8.
180. **Poulter NR**, **Prabhakaran D**, **Caulfield M.** Hypertension. *Lancet* 386: 801–812, 2015. doi:10.1016/S0140-6736(14)61468-9.
181. **Safar ME**, **Asmar R**, **Benetos A**, **Blacher J**, **Boutouyrie P**, **Lacolley P**, **Laurent S**, **London G**, **Pannier B**, **Protogerou A**, **Regnault V**; **French Study Group on Arterial Stiffness.** Interaction between hypertension and arterial stiffness an expert reappraisal. *Hypertension* 72: 796–805, 2018. doi:10.1161/HYPERTENSIONAHA.118.11212.
182. **McEniery CM**, **Yasmin HI**, **Qasem A**, **Wilkinson IB**, **Cockcroft JR.** Normal vascular aging: Differential effects on wave reflection and aortic pulse wave velocity—the Anglo-Cardiff Collaborative Trial (ACCT). *J Am Coll Cardiol* 46: 1753–1760, 2005. doi:10.1016/j.jacc.2005.07.037.
183. **Millasseau SC**, **Guigui FG**, **Kelly RP**, **Prasad K**, **Cockcroft JR**, **Ritter JM**, **Chowienczyk PJ.** Noninvasive assessment of the digital volume pulse: comparison with the peripheral pressure pulse. *Hypertension* 36: 952–956, 2000. doi:10.1161/01.HYP.36.6.952.
184. **Karamanoglu M**, **O'Rourke MF**, **Avolio AP**, **Kelly RP.** An analysis of the relationship between central aortic and peripheral upper limb pressure waves in man. *Eur Heart J* 14: 160–167, 1993. doi:10.1093/eurheartj/14.2.160.
185. **Vlachopoulos C**, **Xaplanteris P**, **Aboyans V**, **Brodmann M**, **Cífková R**, **Cosentino F**, **Carlo MD**, **Gallino A**, **Landmesser U**, **Laurent S**, **Lekakis J**, **Mikhailidis DP**, **Naka KK**, **Protogerou AD**, **Rizzoni D**, **Schmidt-Trucksäss A**, **Van Bortel L**, **Weber T**, **Yamashina A**, **Zimlichman R**, **Boutouyrie P**, **Cockcroft J**, **O'Rourke M**, **Park JB**, **Schillaci G**, **Sillesen H**, **Townsend RR.** The role of vascular biomarkers for primary and secondary prevention. A position paper from the European Society of Cardiology Working Group on peripheral circulation. Endorsed by the Association for Research into. Arterial Structure and Physiology (ARTERY) society. *Atherosclerosis* 241: 507–532, 2015. doi:10.1016/j.atherosclerosis.2015.05.007.
186. **Van Popele NM**, **Grobbee DE**, **Bots ML**, **Asmar R**, **Topouchian J**, **Reneman RS**, **Hoeks APG**, **Van Der Kuip DAM**, **Hofman A**, **Witteman JCM.** Association between arterial stiffness and atherosclerosis: the Rotterdam study. *Stroke* 32: 454–460, 2001. doi:10.1161/01.STR.32.2.454.
187. **Palombo C**, **Kozakova M.** Arterial stiffness, atherosclerosis and cardiovascular risk: Pathophysiologic mechanisms and emerging clinical indications. *Vascul Pharmacol* 77: 1–7, 2016. doi:10.1016/j.vph.2015.11.083.
188. **Song P**, **Rudan D**, **Zhu Y**, **Fowkes FJI**, **Rahimi K**, **Fowkes FGR**, **Rudan I.** Global, regional, and national prevalence and risk factors for peripheral artery disease in 2015: an updated systematic review and analysis. *Lancet Glob Health* 7: e1020–e1030, 2019. doi:10.1016/S2214-109X(19)30255-4.
189. **Conte SM**, **Vale PR.** Peripheral arterial disease. *Hear Lung Circ* 27: 427–432, 2018. doi:10.1016/j.hlc.2017.10.014.
190. **Saleh A**, **Makhamreh H**, **Qoussoos T**, **Alawwa I**, **Alsmady M**, **Salah ZA**, **Shakhatreh A**, **Alhazaymeh L**, **Jabber M.** Prevalence of previously unrecognized peripheral arterial disease in patients undergoing coronary angiography. *Medicine (Baltimore)* 97: e11519, 2018. doi:10.1097/MD.0000000000011519.
191. **Norgren L**, **Hiatt WR**, **Dormandy JA**, **Nehler MR**, **Harris KA**, **Fowkes FGR.** Inter-society consensus for the management of peripheral arterial disease (TASC II). *J Vasc Surg* 45: 5–67, 2007. doi:10.1016/j.jvs.2006.12.037.
192. **O'Rourke MF**, **Pauca A**, **Jiang X-J.** Pulse wave analysis. *Br J Clin Pharmacol* 51: 507–522, 2001. doi:10.1046/j.0306-5251.2001.01400.x.
193. **Avolio AP**, **Butlin M**, **Walsh A.** Arterial blood pressure measurement and pulse wave analysis—their role in enhancing cardiovascular assessment. *Physiol Meas* 31: R1–R47, 2010. doi:10.1088/0967-3334/31/1/R01.
194. **Papaioannou TG**, **Vardoulis O**, **Stergiopulos N.** The "systolic volume balance" method for the noninvasive estimation of cardiac output based on pressure wave analysis. *Am J Physiol Heart Circ Physiol* 302: H2064–H2073, 2012. doi:10.1152/ajpheart.00052.2012.
195. **Monte-Moreno E.** Non-invasive estimate of blood glucose and blood pressure from a photoplethysmograph by means of machine learning techniques. *Artif Intell Med* 53: 127–138, 2011. doi:10.1016/j.artmed.2011.05.001.
196. **Mouney F**, **Tiplica T**, **Hallab M**, **Dinomais M**, **Fasquel J-B.** Towards a smartwatch for cuff-less blood pressure measurement using PPG signal and physiological features. In: *IoT Technologies for HealthCare. HealthyIoT 2019, Lecture Notes of the Institute for Computer Sciences, Social Informatics and Telecommunications Engineering*, edited by Garcia N, Pires I, Goleva R. Cham, Switzerland: Springer, 2020, vol**.** 314, p. 67–76.
197. **Millasseau SC**, **Ritter JM**, **Takazawa K**, **Chowienczyk PJ.** Contour analysis of the photoplethysmographic pulse measured at the finger. *J Hypertens* 24: 1449–1456, 2006. doi:10.1097/01.hjh.0000239277.05068.87.
198. **Murgo JP**, **Westerhof N**, **Giolma JP**, **Altobelli SA.** Aortic input impedance in normal man: relationship to pressure wave forms. *Circulation* 62: 105–116, 1980. doi:10.1161/01.CIR.62.1.105.
199. **Mohanalakshmi S**, **Sivasubramanian A.** Optical sensor system for the non-invasive assessment of arterial stiffness quantified by fourth derivative of photoplethysmogram. *Biomed Eng Appl Basis Commun* 27: 1550021, 2015. doi:10.4015/S1016237215500210.

Downloaded from journals.physiology.org/journal/ajpheart (193.219.170.065) on March 9, 2022.

200. **Kontaxis S**, **Gil E**, **Marozas V**, **Lazaro J**, **Garcia E**, **Posadas-de Miguel M**, **Siddi S**, **Bernal ML**, **Aguilo J**, **Haro JM**, **de la Camara C**, **Laguna P**, **Bailon R.** Photoplethysmographic waveform analysis for autonomic reactivity assessment in depression. *IEEE Trans Biomed Eng* 68: 1273–1281, 2021. doi:10.1109/TBME.2020.3025908.
201. **Erts R**, **Spigulis J**, **Kukulis I**, **Ozols M.** Bilateral photoplethysmography studies of the leg arterial stenosis. *Physiol Meas* 26: 865–874, 2005. doi:10.1088/0967-3334/26/5/022.
202. **Paliakaite B**, **Charlton P**, **Rapalis A**, **Plusciauskaite V**, **Piartli P**, **Kaniusas E**, **Marozas V.** *Blood pressure estimation based on photoplethysmography: finger versus wrist. 2021 Computing in Cardiology (CinC)*. Brno, Czech Republic, September 13–15, 2021, p. 1–4.
203. **Chan C**, **Hosanee W**, **Kyriacou Z**, **Allen A**, **Lovell FE.** Multi-site photoplethysmography technology for blood pressure assessment: challenges and recommendations. *J Clin Med* 8: 1827, 2019. doi:10.3390/jcm8111827.
204. **Willemet M**, **Chowienczyk P**, **Alastruey J.** A database of virtual healthy subjects to assess the accuracy of foot-to-foot pulse wave velocities for estimation of aortic stiffness. *Am J Physiol Heart Circ Physiol* 309: H663–H675, 2015. doi:10.1152/ajpheart.00175.2015.
205. **Allen J**, **Murray A.** Similarity in bilateral photoplethysmographic peripheral pulse wave characteristics at the ears, thumbs and toes. *Physiol Meas* 21: 369–377, 2000. doi:10.1088/0967-3334/21/3/303.
206. **Kim HL**, **Kim SH.** Pulse wave velocity in atherosclerosis. *Front Cardiovasc Med* 6: 41, 2019. doi:10.3389/fcvm.2019.00041.
207. **Welykholowa K**, **Hosanee M**, **Chan G**, **Cooper R**, **Kyriacou PA**, **Zheng D**, **Allen J**, **Abbott D**, **Menon C**, **Lovell NH**, **Howard N**, **Chan W**, **Lim K**, **Fletcher R**, **Ward R**, **Elgendi M.** Multimodal photoplethysmography-based approaches for improved detection of hypertension. *J Clin Med* 9: 1203, 2020. doi:10.3390/jcm9041203.
208. **Ding XR**, **Zhao N**, **Yang GZ**, **Pettigrew RI**, **Lo B**, **Miao F**, **Li Y**, **Liu J**, **Zhang YT.** Continuous blood pressure measurement from invasive to unobtrusive: celebration of 200th birth anniversary of Carl Ludwig. *IEEE J Biomed Health Inform* 20: 1455–1465, 2016. doi:10.1109/JBHI.2016.2620995.
209. **Yoshioka M**, **Bounyong S.** *Regression-forests-based estimation of blood pressure using the pulse transit time obtained by facial photoplethysmogram. 2017 International Joint Conference on Neural Networks (IJCNN)*, Anchorage, AK, May 14–19, 2017, p. 3248–3253.
210. **Balmer J**, **Pretty C**, **Davidson S**, **Desaive T**, **Kamoi S**, **Pironet A**, **Morimont P**, **Janssen N**, **Lambermont B**, **Shaw GM**, **Chase JG.** Pre-ejection period, the reason why the electrocardiogram Q-wave is an unreliable indicator of pulse wave initialization. *Physiol Meas* 39: 095005, 2018. doi:10.1088/1361-6579/aada72.
211. **Mukundan L**, **Kayalvizhi N.** *Age dependence of pulse transit time derived from dual PPGs and PPG-ECG duo—a comparative study. 2017 14th IEEE India Council International Conference (INDICON)*, Roorkee, India, December 15–17, 2017, p. 1–4. doi:10.1109/INDICON.2017.8487630.
212. **Shao D**, **Yang Y**, **Tsow F**, **Liu C**, **Tao N.** *Non-Contact Simultaneous Photoplethysmogram and Ballistocardiogram Video Recording towards Real-Time Blood Pressure and Abnormal Heart Rhythm Monitoring. 2017 12th IEEE International Conference on Automatic Face & Gesture Recognition (FG 2017)*, Washington, DC, 2017, p. 273–277.
213. **Kamboj N**, **Chang K**, **Metcalfe K**, **Chu CH**, **Conway A.** Accuracy and precision of continuous non-invasive arterial pressure monitoring in critical care: a systematic review and meta-analysis. *Intensive Crit Care Nurs* 67: 103091, 2021. doi:10.1016/j.iccn.2021.103091.
214. **Holz C**, **Wang EJ.** Glabella: continuously sensing blood pressure behavior using an unobtrusive wearable device. *Proc ACM Interactive Mobile Wearable Ubiquitous Technol* 1: 1–23, 2017. doi:10.1145/3132024.
215. **Panchangam C**, **Merrill ED**, **Raghuveer G.** Utility of arterial stiffness assessment in children. *Cardiol Young* 28: 362–376, 2018. doi:10.1017/S1047951117002402.
216. **Bland JM**, **Altman DG.** Statistical methods for assessing agreement between two methods of clinical measurement. *Lancet* 1: 307–310, 1986. doi:10.1016/S0140-6736(86)90837-8.
217. **Stergiou GS**, **Alpert B**, **Mieke S**, **Asmar R**, **Atkins N**, **Eckert S**, **Frick G**, **Friedman B**, **Graßl T**, **Ichikawa T**, **Ioannidis JP**, **Lacy P**, **McManus R**, **Murray A**, **Myers M**, **Palatini P**, **Parati G**, **Quinn D**, **Sarkis J**, **Shennan A**, **Usuda T**, **Wang J**, **Wu CO**, **O'Brien E.** A universal standard for the validation of blood pressure measuring devices: Association for the Advancement of Medical Instrumentation/European Society of Hypertension/International Organization for Standardization (AAMI/ESH/ISO) Collaboration Statement. *Hypertension* 71: 368–374, 2018. doi:10.1161/HYPERTENSIONAHA.117.10237.
218. **Christodoulou E**, **Ma J**, **Collins GS**, **Steyerberg EW**, **Verbakel JY**, **Van Calster B.** A systematic review shows no performance benefit of machine learning over logistic regression for clinical prediction models. *J Clin Epidemiol* 110: 12–22, 2019. doi:10.1016/j.jclinepi.2019.02.004.
219. **Bartlett JW**, **Frost C.** Reliability, repeatability and reproducibility: analysis of measurement errors in continuous variables. *Ultrasound Obstet Gynecol* 31: 466–475, 2008. doi:10.1002/uog.5256.
220. **Tahvanainen A**, **Leskinen M**, **Koskela J**, **Ilveskoski E**, **Alanko J**, **Kähönen M**, **Kööbi T**, **Lehtimäki L**, **Moilanen E**, **Mustonen J**, **Pörsti I.** Non-invasive measurement of the haemodynamic effects of inhaled salbutamol, intravenous L-arginine and sublingual nitroglycerin. *Br J Clin Pharmacol* 68: 23–33, 2009. doi:10.1111/j.1365-2125.2009.03434.x.
221. **Jobbágy A**, **Csordás P**, **Mersich A.** Blood pressure measurement: assessment of a variable quantity. *Zdr Vestn* 80: 316–324, 2011. doi:10.6016/87.
222. **Avram R**, **Olgin JE**, **Kuhar P**, **Hughes JW**, **Marcus GM**, **Pletcher MJ**, **Aschbacher K**, **Tison GH.** A digital biomarker of diabetes from smartphone-based vascular signals. *Nat Med* 26: 1576–1582, 2020. doi:10.1038/s41591-020-1010-5.
223. **Harmon QE**, **Huang L**, **Umbach DM**, **KlungsØyr K**, **Engel SM**, **Magnus P**, **Skjærven R**, **Zhang J**, **Wilcox AJ.** Risk of fetal death with preeclampsia. *Obstet Gynecol* 125: 628–635, 2015. doi:10.1097/AOG.0000000000000696.
224. **Sudlow C**, **Gallacher J**, **Allen N**, **Beral V**, **Burton P**, **Danesh J**, **Downey P**, **Elliott P**, **Green J**, **Landray M**, **Liu B**, **Matthews P**, **Ong G**, **Pell J**, **Silman A**, **Young A**, **Sprosen T**, **Peakman T**, **Collins R.** UK Biobank: an open access resource for identifying the causes of a wide range of complex diseases of middle and old age. *PLoS Med* 12: e1001779, 2015. doi:10.1371/journal.pmed.1001779.
225. **Johnson AEW**, **Pollard TJ**, **Shen L**, **Lehman LH**, **Feng M**, **Ghassemi M**, **Moody B**, **Szolovits P**, **Anthony Celi L**, **Mark RG.** MIMIC-III, a freely accessible critical care database. *Sci Data* 3: 160035, 2016. doi:10.1038/sdata.2016.35.
226. **Kachuee M**, **Kiani MM**, **Mohammadzade H**, **Shabany M.** Cuffless blood pressure estimation algorithms for continuous health-care monitoring. *IEEE Trans Biomed Eng* 64: 859–869, 2017. doi:10.1109/TBME.2016.2580904.
227. **Kachuee M**, **Kiani MM**, **Ohammadzade H**, **Shabany M.** Cuff-less high-accuracy calibration-free blood pressure estimation using pulse transit time. *2015 IEEE International Symposium on Circuits and Systems (ISCAS)*, Lisbon, Portugal, May 24–27, 2015, p. 1006–1009.
228. **Liang Y**, **Chen Z**, **Liu G**, **Elgendi M.** A new, short-recorded photoplethysmogram dataset for blood pressure monitoring in China. *Sci Data* 5: 180020, 2018. doi:10.1038/sdata.2018.20.
229. **Liu D**, **Görges M**, **Jenkins SA.** University of Queensland vital signs dataset: development of an accessible repository of anesthesia patient monitoring data for research. *Anesth Analg* 114: 584–589, 2012. doi:10.1213/ANE.0b013e318241f7c0.
230. **Charlton PH**, **Mariscal Harana J**, **Vennin S**, **Li Y**, **Chowienczyk P**, **Alastruey J.** Pulse Wave Database (PWDB): a Database of Arterial Pulse Waves Representative of Healthy Adults (Online). *Zenodo*, 2019. doi:10.5281/zenodo.2633174. [Last accessed, 13 Feb 2022].
231. **Hosanee M**, **Chan G**, **Welykholowa K**, **Cooper R**, **Kyriacou PA**, **Zheng D**, **Allen J**, **Abbott D**, **Menon C**, **Lovell NH**, **Howard N**, **Chan W**, **Lim K**, **Fletcher R**, **Ward R**, **Elgendi M.** Cuffless single-site photoplethysmography for blood pressure monitoring. *J Clin Med* 9: 723, 2020. doi:10.3390/jcm9030723.
232. **Charlton PH.** PulseAnalyse: a Signal Processing Tool for Cardiovascular Pulse Waves (Online). Zenodo, 2019. http://doi.org/10.5281/zenodo.3272122. [Last accessed, 13 Feb 2022].
233. **Gaddum N.** TTAlgorithm (Online). MathWorks File Exchange. http://www.mathworks.co.uk/matlabcentral/fileexchange/37746-ttalgorithm [2022 Feb 1].
234. **Mishra T**, **Wang M**, **Metwally AA**, **Bogu GK**, **Brooks AW**, **Bahmani A**, **Alavi A**, **Celli A**, **Higgs E**, **Dagan-Rosenfeld O**, **Fay B**, **Kirkpatrick S**, **Kellogg R**, **Gibson M**, **Wang T**, **Hunting EM**, **Mamic P**, **Ganz AB**, **Rolnik B**, **Li X**, **Snyder MP.** Pre-symptomatic detection of COVID-19 from smartwatch data. *Nat Biomed Eng* 4: 1208–1220, 2020. doi:10.1038/s41551-020-00640-6.

Downloaded from journals.physiology.org/journal/ajpheart (193.219.170.065) on March 9, 2022.

235. **Quer G**, **Radin JM**, **Gadaleta M**, **Baca-Motes K**, **Ariniello L**, **Ramos E**, **Kheterpal V**, **Topol EJ**, **Steinhubl SR.** Wearable sensor data and self-reported symptoms for COVID-19 detection. *Nat Med* 27, 2020. doi:10.1038/s41591-020-1123-x.
236. **Chatterjee S**, **Budidha K**, **Kyriacou PA.** Investigating the origin of photoplethysmography using a multiwavelength Monte Carlo model. *Physiol Meas* 41: 084001, 2020. doi:10.1088/1361-6579/aba008.
237. **Charlton PH**, **Kyriacou P**, **Mant J**, **Alastruey J.** Acquiring wearable photoplethysmography data in daily life: the PPG Diary Pilot Study. *Eng Proc* 2: 80, 2020. doi:10.3390/ecsa-7-08233.
238. **Natarajan A**, **Pantelopoulos A**, **Emir-Farinas H**, **Natarajan P.** Heart rate variability with photoplethysmography in 8 million individuals: a cross-sectional study. *Lancet Digit Health* 2: e650–e657, 2020. doi:10.1016/S2589-7500(20)30246-6.
239. **McKay ND**, **Griffiths B**, **Di Maria C**, **Hedley S**, **Murray A**, **Allen J.** Novel photoplethysmography cardiovascular assessments in patients with Raynaud's phenomenon and systemic sclerosis: a pilot study. *Rheumatol (United Kingdom)* 53: 1855–1863, 2014. doi:10.1093/rheumatology/keu196.
240. **Babrak LM**, **Menetski J**, **Rebhan M**, **Nisato G**, **Zinggeler M**, **Brasier N**, **Baerenfaller K**, **Brenzikofer T**, **Baltzer L**, **Vogler C**, **Gschwind L**, **Schneider C**, **Streiff F**, **Groenen PMA**, **Miho E.** Traditional and digital biomarkers: two worlds apart? *Digit Biomark* 3: 92–102, 2019. doi:10.1159/000502000.
241. **Huthart S**, **Elgendi M**, **Zheng D**, **Stansby G**, **Allen J.** Advancing PPG signal quality and know-how through knowledge translation—from experts to student and researcher. *Front Digit Health* 2: 619692, 2020. doi:10.3389/fdgth.2020.619692.
242. **Passler S**, **Müller N**, **Senner V.** In-ear pulse rate measurement: a valid alternative to heart rate derived from electrocardiography? *Sensors* 19: 3641, 2019. doi:10.3390/s19173641.
243. **Chan PH**, **Wong CK**, **Poh YC**, **Pun L**, **Leung WWC**, **Wong YF**, **Wong MMY**, **Poh MZ**, **Chu DWS**, **Siu CW.** Diagnostic performance of a smartphone-based photoplethysmographic application for atrial fibrillation screening in a primary care setting. *J Am Heart Assoc* 5: e003428, 2016. doi:10.1161/JAHA.116.003428.
244. **Dawber TR**, **Thomas HE**, **McNamara PM.** Characteristics of the dicrotic notch of the arterial pulse wave in coronary heart disease. *Angiology* 24: 244–255, 1973. doi:10.1177/000331977302400407.
245. **Charlton PH**, **Bonnici T**, **Tarassenko L**, **Alastruey J**, **Clifton DA**, **Beale R**, **Watkinson PJ.** Extraction of respiratory signals from the electrocardiogram and photoplethysmogram: technical and physiological determinants. *Physiol Meas* 38: 669–690, 2017. doi:10.1088/1361-6579/aa670e.
246. **Charlton PH**, **Kyriacou P**, **Mant J**, **Marozas V**, **Chowienczyk P**, **Alastruey J.** Wearable photoplethysmography for cardiovascular monitoring. *Proceedings of the IEEE*. 110:3, 2022. doi:10.1109/JPROC.2022.3149785.

Downloaded from journals.physiology.org/journal/ajpheart (193.219.170.065) on March 9, 2022.